Lasers. Metal vapor laser.
High speed imaging based on the laser type.

Maxim. V. Trigub

Institute of Atmospheric Optics SB RAS, 1 Zuev Sq., 634055, Tomsk, Russia;
Tomsk Polytechnic University, 30 Lenina av., 634050, Tomsk, Russia

Scientific team: **Shiyanov D.V., Vasnev N.A., Gembukh P.I.,**
Semenov K.Yu.

Outline

1. What is the laser?
2. Metal vapor laser.
3. Pumping sources and the principle of operation.
4. Operating in the superradiance mode (Amplified spontaneous emission mode).
5. The main properties.
6. Laser active optical systems. Types, principle of operation.
7. Some points of the application.

Laser

N. Basov
1922–2001

A. Prokhorov
1916–2002

H. Townes
1915–2015

In 1951 Charles H. Townes, then at Columbia University in New York City, thought of a way to generate stimulated emission at microwave frequencies. At the end of 1953, he demonstrated a working device that focused “excited” (see below Energy levels and stimulated emissions) ammonia molecules in a resonant microwave cavity, where they emitted a pure microwave frequency. Townes named the device a maser, for “microwave amplification by the stimulated emission of radiation.” Aleksandr Mikhaylovich Prokhorov and Nikolay Gennadiyevich Basov of the P.N. Lebedev Physical Institute in Moscow independently described the theory of maser operation. For their work all three shared the 1964 Nobel Prize for Physics.

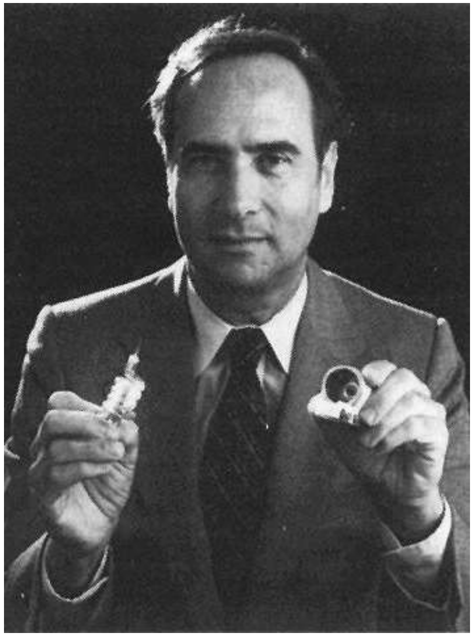

T. Maiman
1927–2007

He fired bright pulses from a photographer's flash lamp to excite chromium atoms in a crystal of synthetic ruby, a material he chose because he had studied carefully how it absorbed and emitted light and calculated that it should work as a laser. On May 16, 1960, he produced red pulses from a ruby rod about the size of a fingertip. In December 1960 Ali Javan, William Bennett, Jr., and Donald Herriott at Bell Labs built the first gas laser, which generated a continuous infrared beam from a mixture of helium and neon. In 1962 Robert N. Hall and coworkers at the General Electric Research and Development Center in Schenectady, New York, made the first semiconductor laser.

Energy levels and stimulated emissions

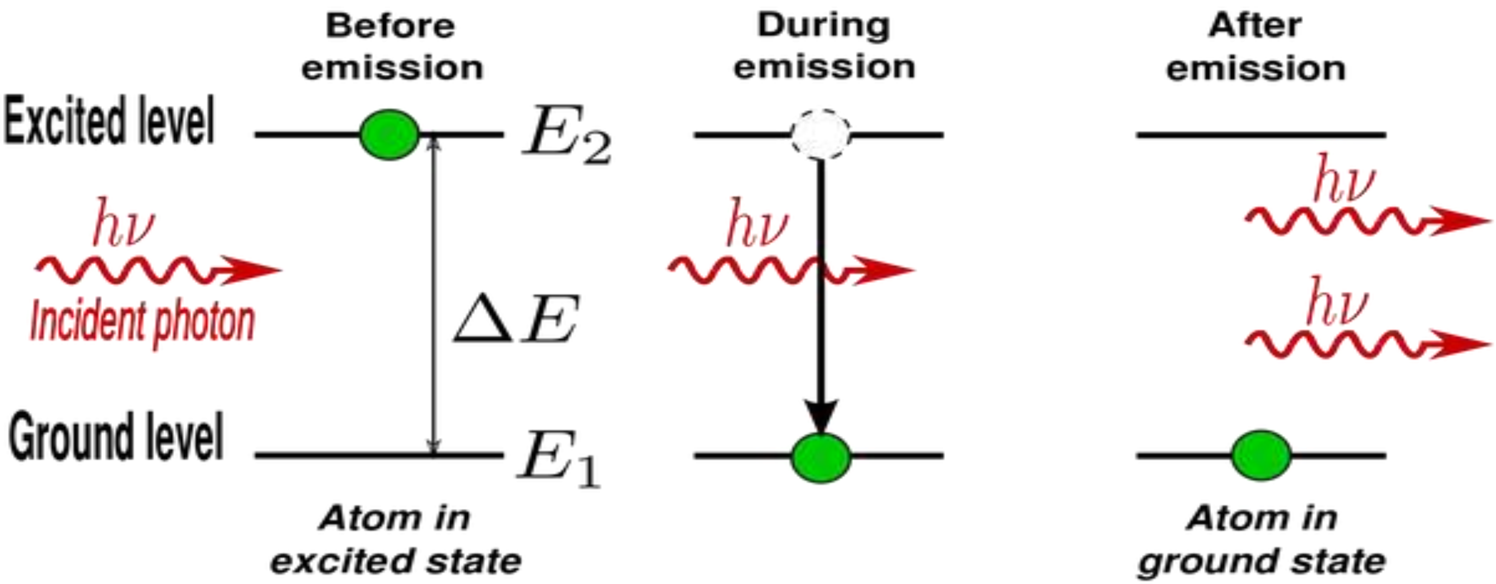

$$E_2 - E_1 = \Delta E = h\nu$$

Energy levels and stimulated emissions

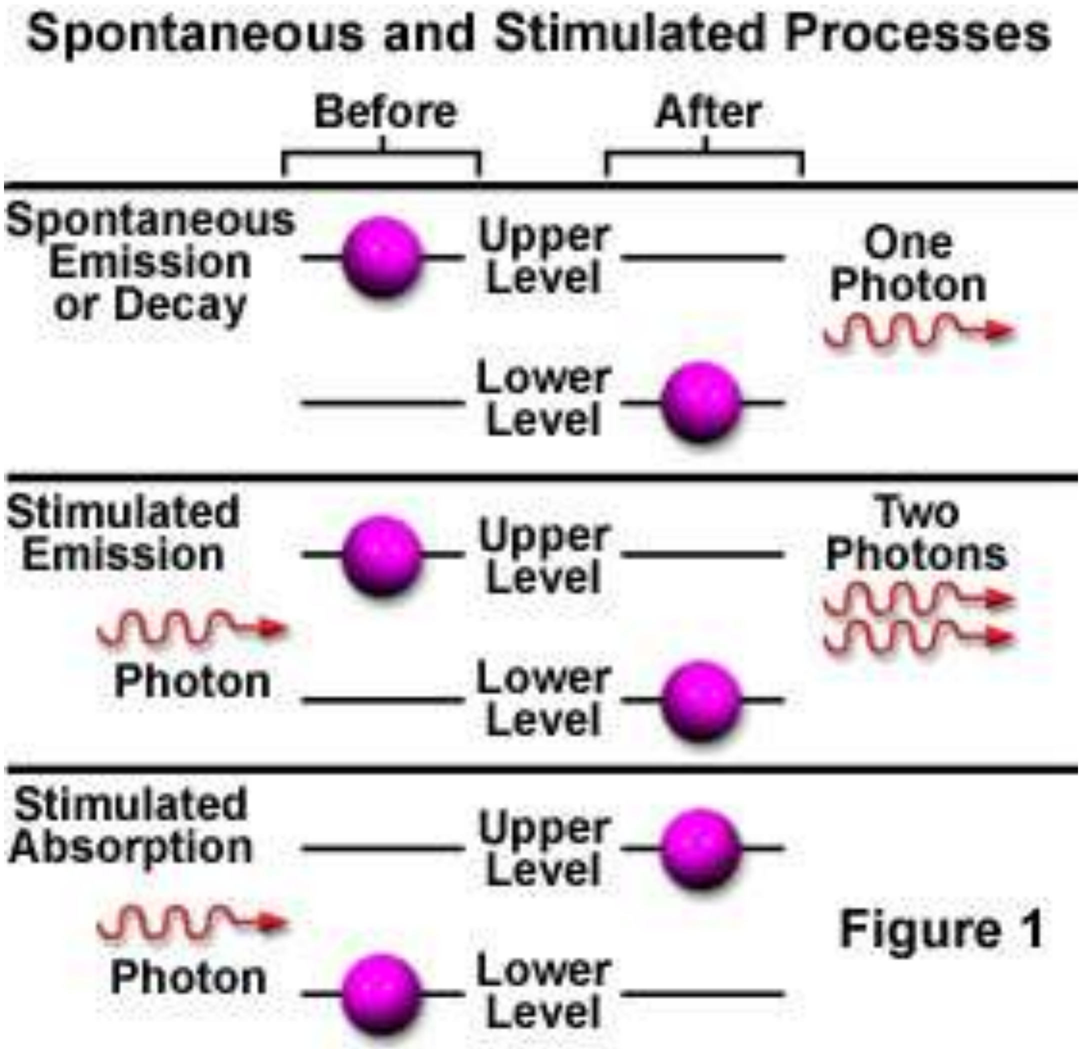

Energy levels and stimulated emissions

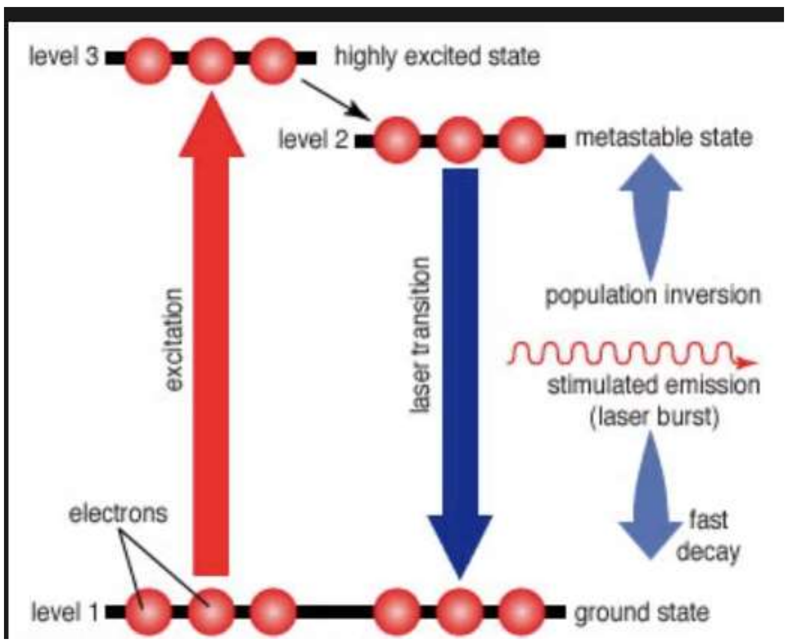

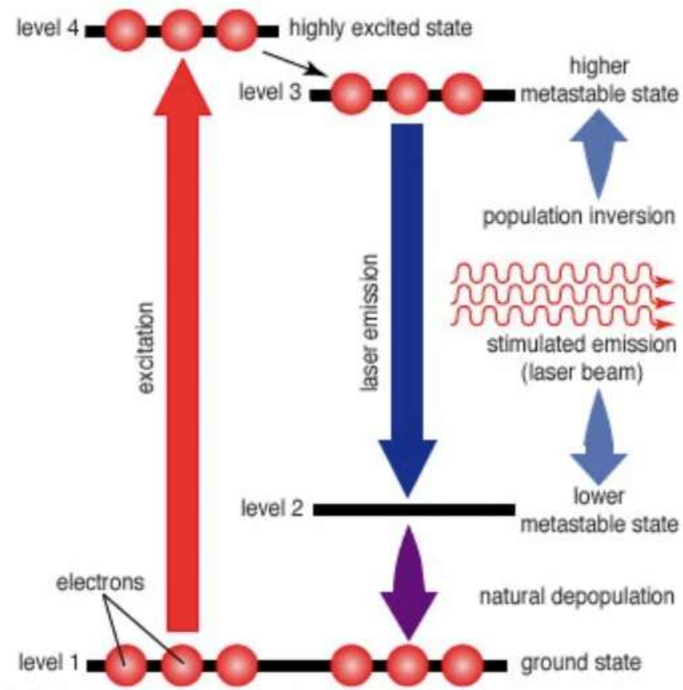

Principle of operation

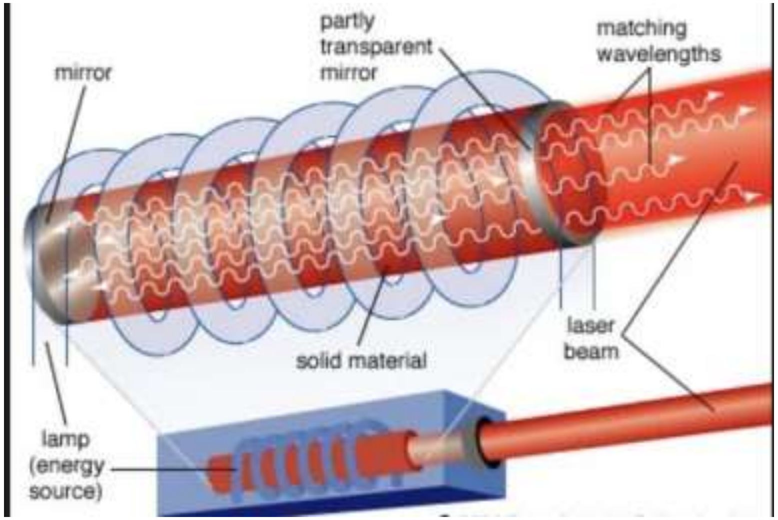

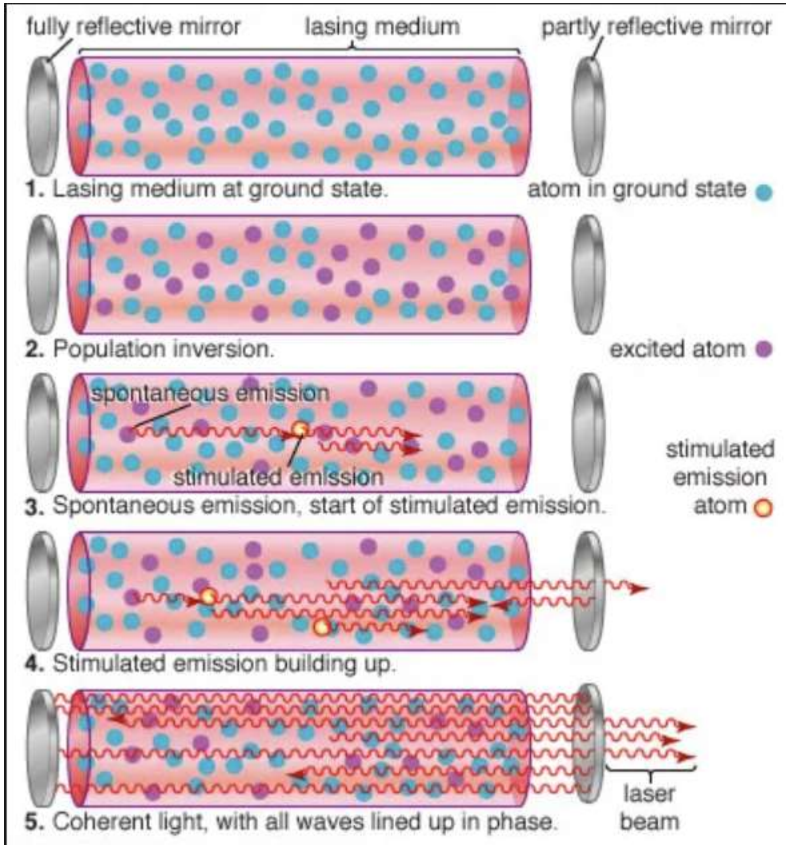

The aim of the work

Real-time imaging of fast processes blocked from viewing by the background radiation:

•*Self-propagating high-temperature synthesis (SHS)*

•*Production of nanoscale structures*

•*Laser processing of materials*

•*Welding process*

•*Interaction of energy flows with biological objects*

•*Remote object imaging*

•*etc.*

Processing (converting) of the optical signals with an adjusted contrast

Challenge

To find the medium for optical signal converting

- *In different spectral ranges*
- *With low distortions*
- *With high-time resolution*

Relevance of the work

The development of methods and tools for high-speed visualization is an important task, the solution of which makes it possible to study fast processes [1-4].

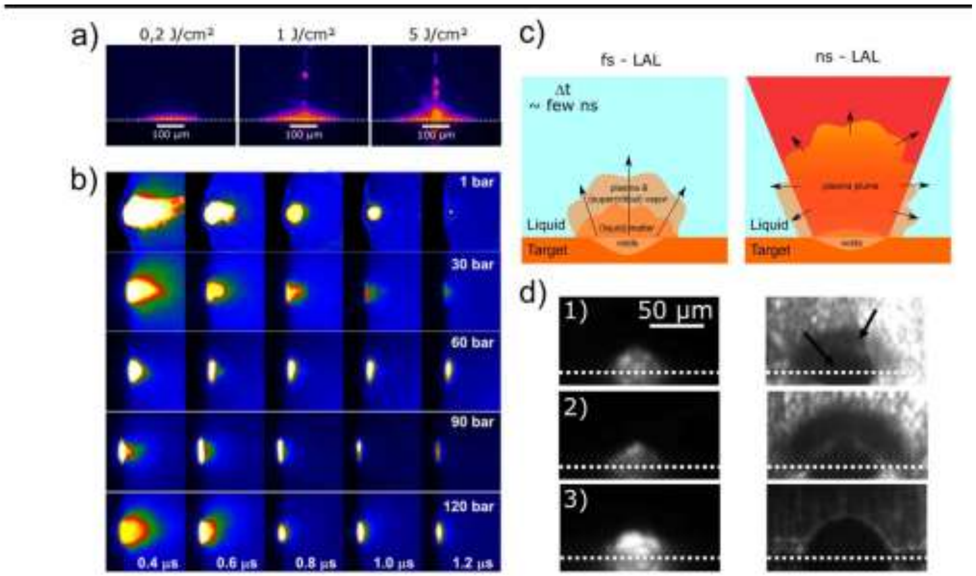

Figure 6. Plasma formation and appearance of the plasma induced by LAL at different time scales. (a) Plasma imaging of fs-LAL of i water for different fluences. (Reproduced from [64]) (b) Plasma imaging of ns-LAL of silver for different pressures in water. (Repro from [163].) (c) Schematic of fs- and ns-LAL. In contrast to fs-LAL, the plasma plume interacts with the laser beam resulting in fu plasma excitation (and plasma shielding). The arrows indicate the direction of energy flow, which for fs-LAL results from the target s towards the bulk liquid whereas for ns-LAL the laser-plasma interaction leads to an energy deposition farther away from the target. (d) Plasma imaging and shadow imaging to display the cavitation bubble boundary for different laser pulse duration at a time delay intensity maximum of the pulse. The upper image was taken for a 19 ns laser pulse. The middle image for a 50 ns laser pulse and the image for a 100 ns laser pulse. For the 19 ns laser pulse, the plasma exceeds the boundary of the cavitation bubble. For the 50 ns pul plasma boundary coincides with the cavitation bubble boundary. For the 100 ns pulse, the cavitation bubble boundary exceeds the p boundary. (Reproduced from [66].)

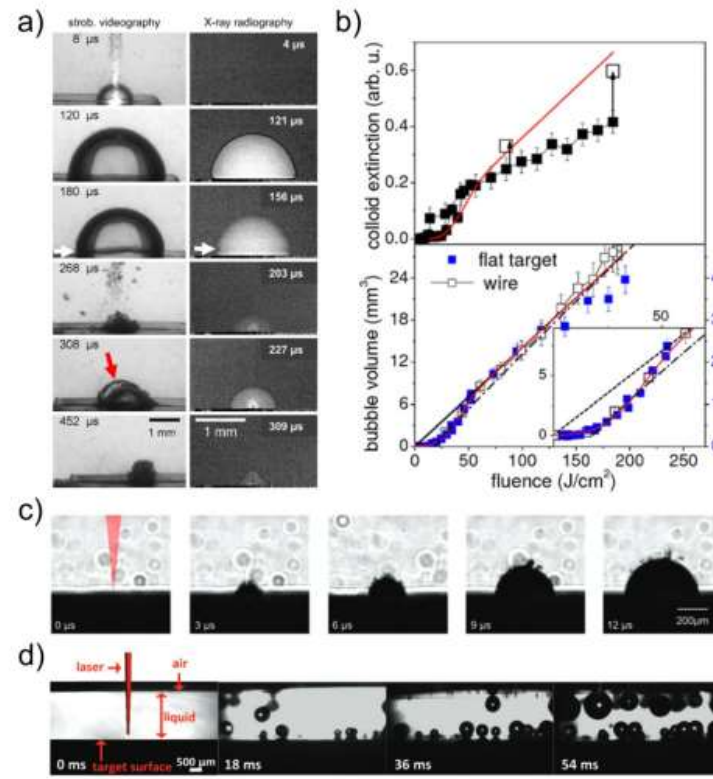

Figure 10. Properties of the cavitation bubble. (a) Stroboscopic videography (left column) and x-ray radiography (right column) images of the cavitation bubble evolution induced by LAL on a silver target immersed in water as a function of delay after laser irradiation indicating the formation of a rim (white arrows) and the depression of the liquid (red arrow). After the first (delay time of 203 μs) and second rebound (delay time of 309 μs) asymmetric shape deviations from the initial quasi-hemispherically cavitation bubble are observed (Reprinted with permission from [209], Copyright 2017 Elsevier). (b) Colloid extinction representing the mass concentration after 150 laser shots and bubble volumes produced by LAL of a flat (right y-axis) and wire (left y-axis) silver target depended on the applied laser fluence. (Reprinted with permission from [210], Copyright 2017 WileyVCH Verlag GmbH & Co. KGaA, Weinheim). (c) Appearance of satellite microbubbles around the cavitation bubble after single-laser pulse (2 ps) irradiation of a gold target (Reprinted with permission from [39], Copyright 2018 The Royal Society of Chemistry). (d) Formation of persistent micro-bubbles milliseconds after LAL of a gold target in water (Reproduced from [78] with permission from the PCCP Owner Societies).

1. Kanitz A., Kalus M.R., Gurevich E.L., Ostendorf A., Barcikowski S., Amans D. Review on experimental and theoretical investigations of the early stage, femtoseconds to microseconds processes during laser ablation in liquid-phase for the synthesis of colloidal nanoparticles // Plasma Sources Science and Technology. – 2019. – Vol. 28. № 10.
2. Dittrich S., Barcikowski S., Gökce B. Plasma and nanoparticle shielding during pulsed laser ablation in liquids cause ablation efficiency decrease // Opto-Electronic Advances. – 2021. – Vol. 4, – № 1. – P. 200072–1.
3. Amendola V., Amans D., Ishikawa Y., Koshizaki N., Scirè S., Compagnini G., Reichenberger S., Barcikowski S. Room-Temperature Laser Synthesis in Liquid of Oxide, Metal-Oxide Core-Shells, and Doped Oxide Nanoparticles // Chemistry - A European Journal. – 2020. – Vol. 26, – № 42. – P. 9206–9242.
4. Chemin A., Fawaz M.W., Amans D. Investigation of the blast pressure following laser ablation at a solid–fluid interface using shock waves dynamics in air and in water // Applied Surface Science. – 2022. – Vol. 574. – DOI: 10.1016/J.APSUSC.2021.151592

Relevance of the work

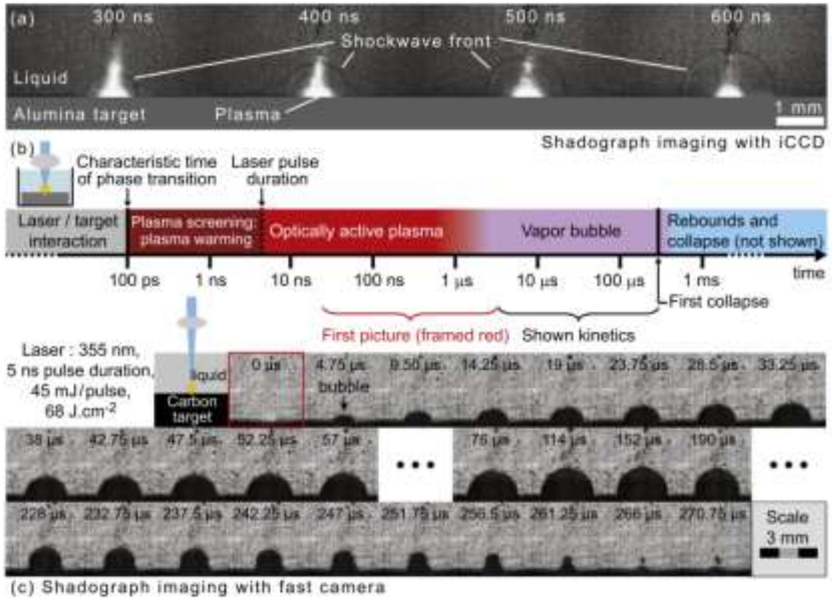

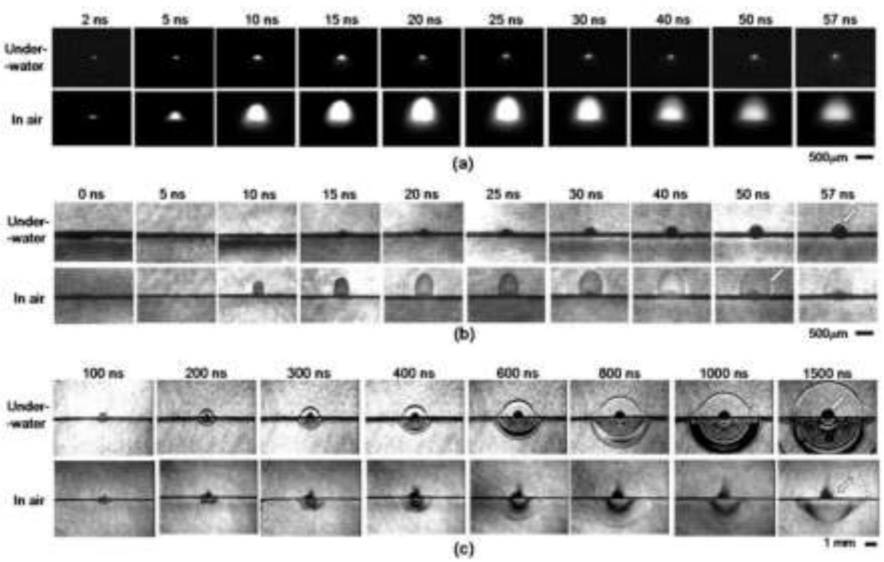

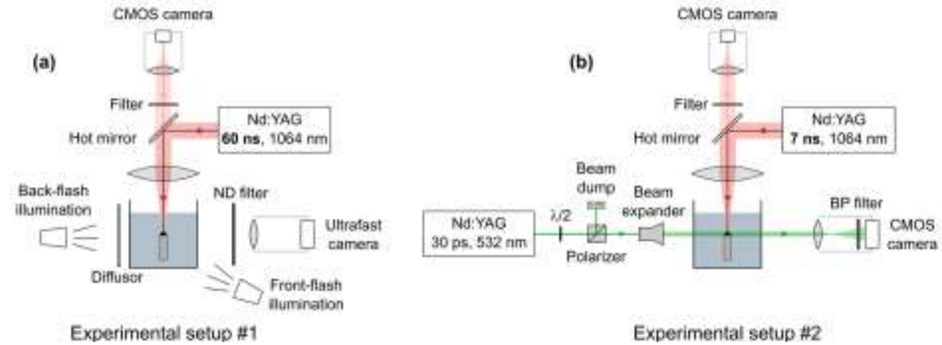

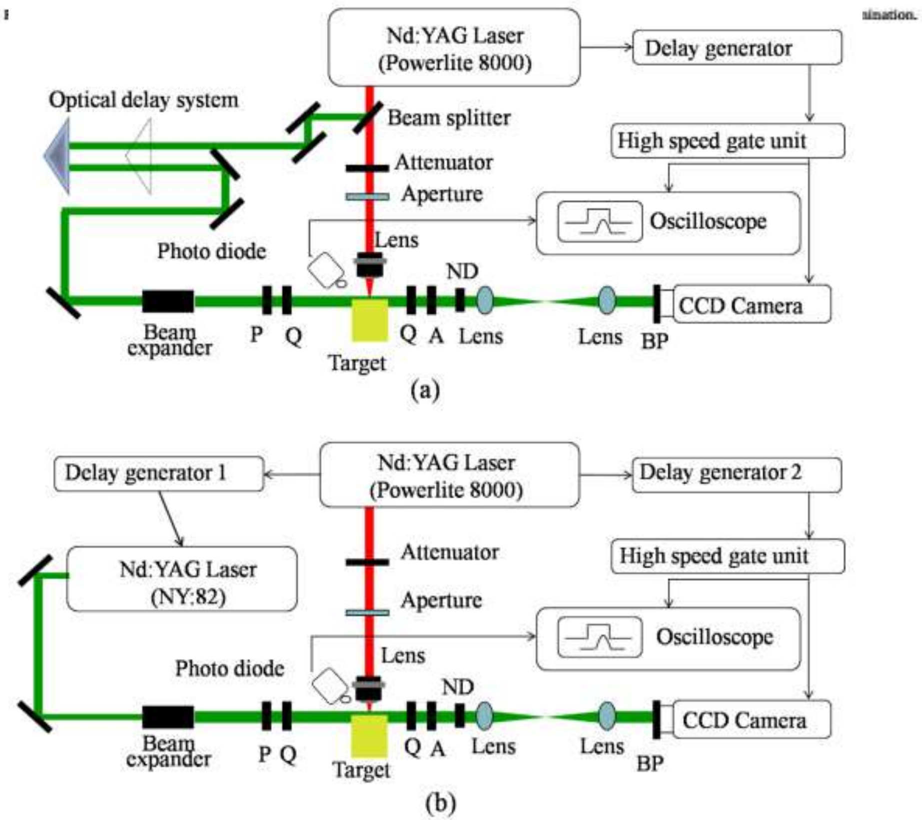

1. Amans D., Diouf M., Lam J., Ledoux G., Dujardin C. Origin of the nano-carbon allotropes in pulsed laser ablation in liquids synthesis // Journal of Colloid and Interface Science. – 2017. – Vol. 489. – P. 114–125. – DOI: 10.1016/J.JCIS.2016.08.017.

2.Nguyen T.T.P., Tanabe R., Ito Y. Comparative study of the expansion dynamics of laser-driven plasma and shock wave in in-air and underwater ablation regimes // Optics and Laser Technology. – 2018. – Vol. 100. – P. 21–26. – DOI: 10.1016/J.OPTLASTEC.2017.09.021.

Relevance of the work

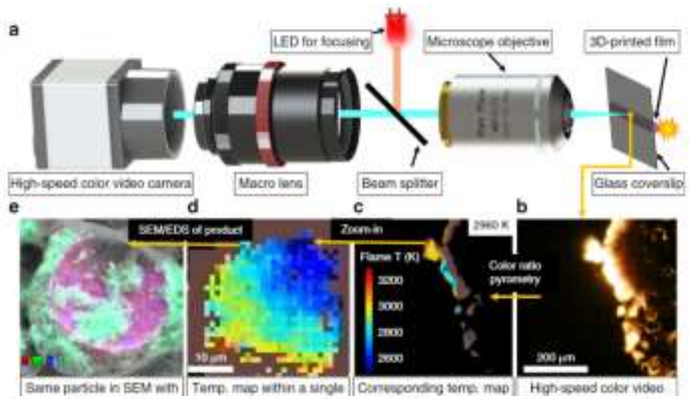

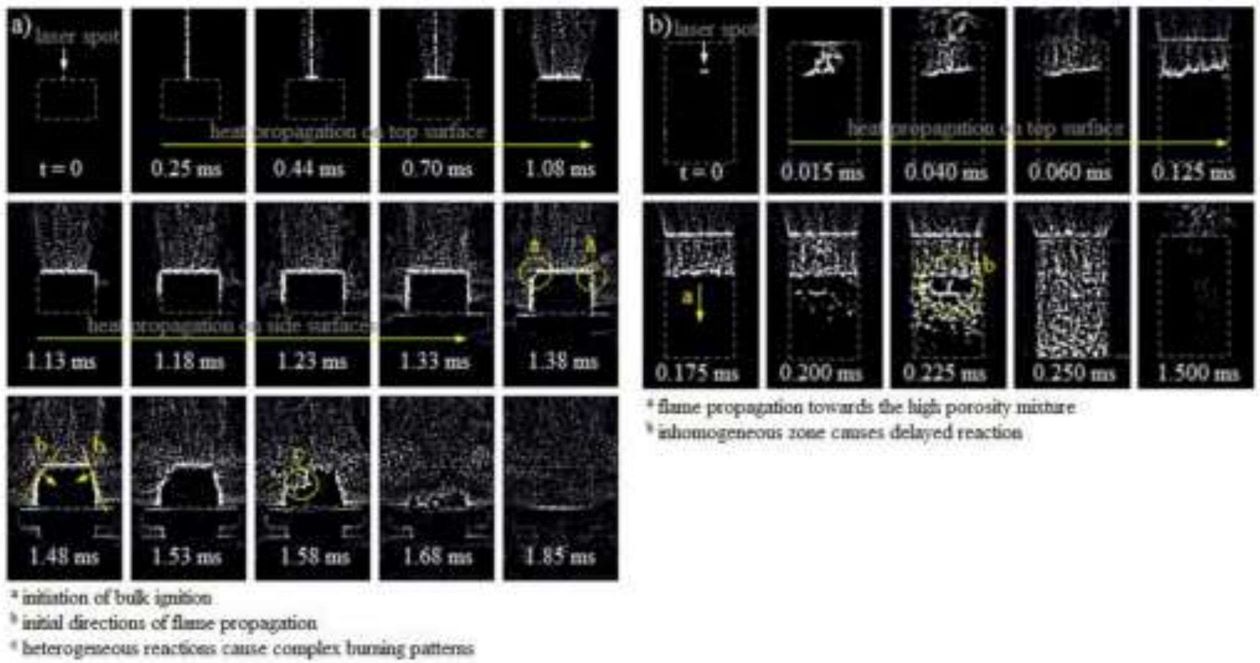

FIGURE 3 | High speed frames of the ignition and propagation of the burn front within the Al/CuO mixtures for **(a)** pellet, and **(b)** lightly packed powder.

1. Wang H., Kline D.J., Zachariah M.R. In-operando high-speed microscopy and thermometry of reaction propagation and sintering in a nanocomposite // Nature Communications. – 2019. – Vol. 10, – № 1.
2.Saceleanu F., Idir M., Chaumeix N., Wen J.Z. Combustion characteristics of physically mixed 40 nm aluminum/copper oxide nanothermites using laser ignition // Frontiers in Chemistry. – 2018. – Vol. 6, – № SEP.

High-speed imaging

Laser illumination method

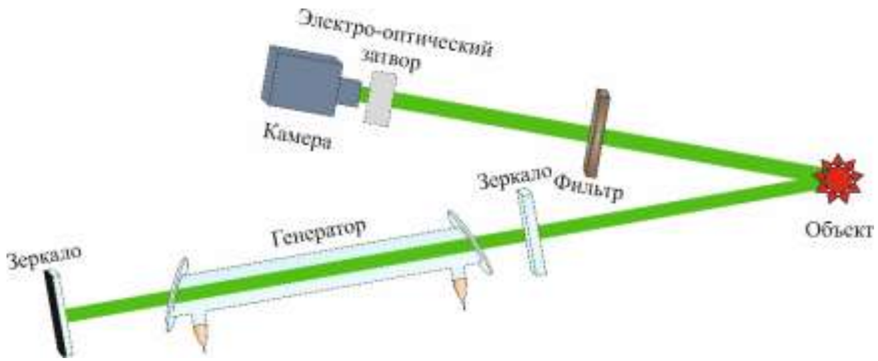

Requirements:
- Low Beam Divergence;
- High radiation intensity at the object;
- Small filter transmission width (nm units);

Advantages:
- Compact implementation.

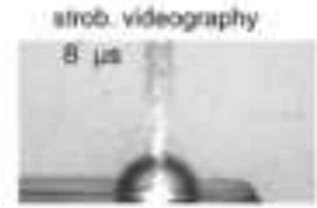

Introduction

Necessary pressure of work substance

Evaporation of metal halides

Evaporation of metals

Power of pump pulses

Power of pump pulses

Molecule dissociation

Atom excitation

(Cu – 510,6 and 578,2 nm)

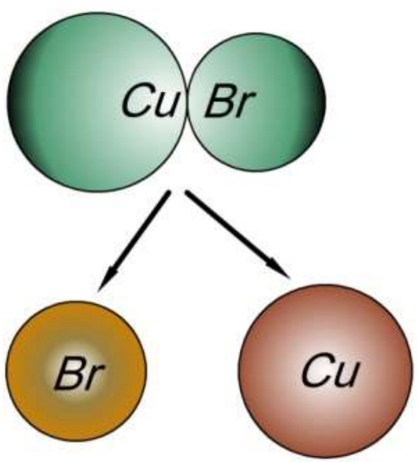

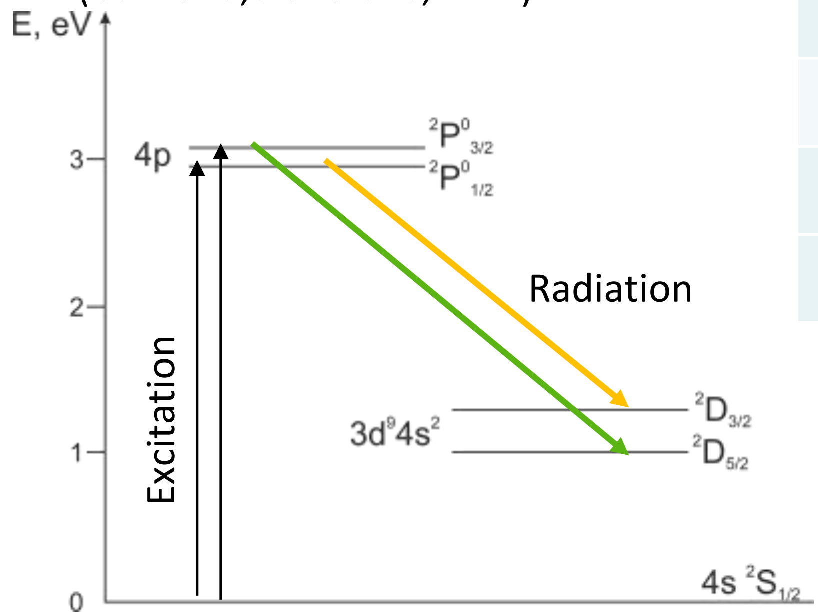

Metal	T,°C
Copper	≃1450
Lead	≃950
Strontium	≃800
Manganese	≃1350

Approximate temperature of active zone

The design of self-heated metal vapor laser

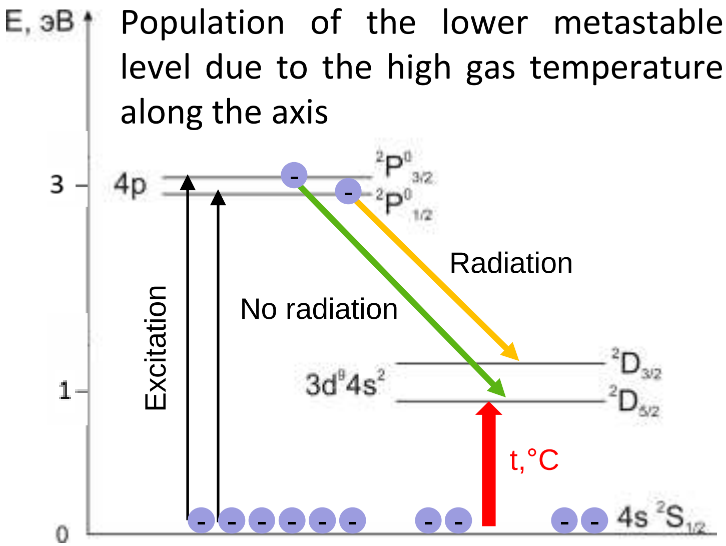

Population of the lower metastable level due to the high gas temperature along the axis

Limitations:

1. Metal is located in the discharge zone.

2. The concentration of metal atoms can't be changed without active zone temperature variation.

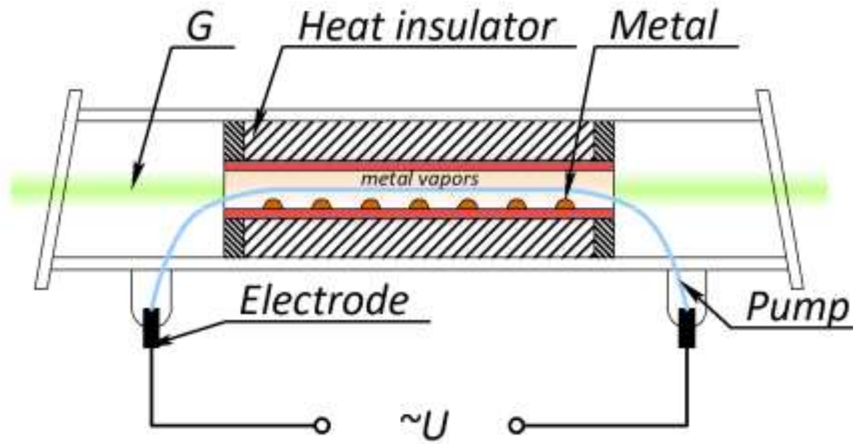

Low pump power, low active zone temperature, low radiation (G)

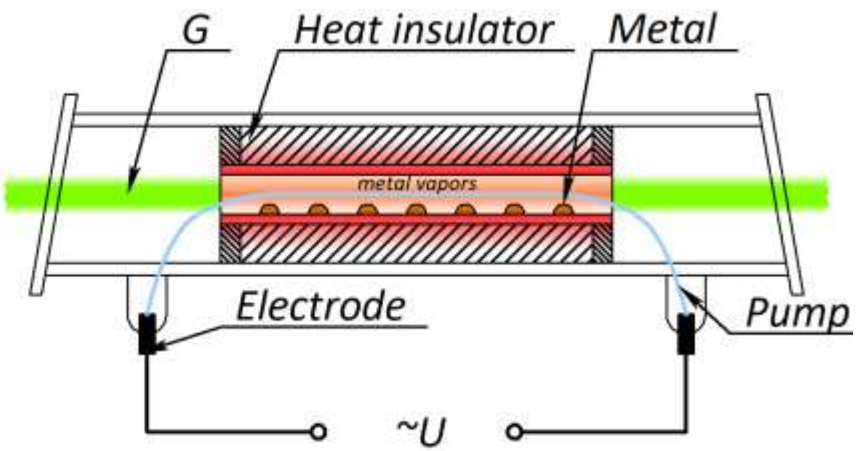

High pump power, high active zone temperature, high radiation (G)

The design of the active element with inductor dispenser

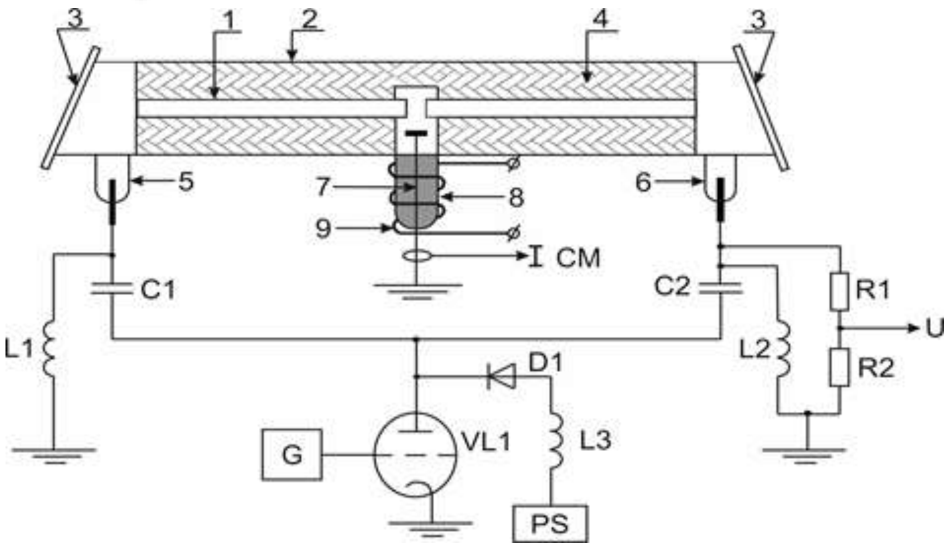

The design of the active element and the pilot plant: 1 – discharge channel, 2 – quartz vacuum tube, 3 – windows, 4 – heat insulator (ZrO2), 5 and 6 – cathode electrodes of the left and right sections, 7 - anode electrode, 8 - dispenser of vapor of the working substance (copper), 9 – inductor, G – control pulse generator, PS – power supply.

Advantage:
This design allow to separate the functions of the production and excitation of vapors between different sources

Limitations:
need to use the pump source for heating and maintaining the active media temperature

Other methods to get metal vapors [1]:

- Self-heating
- Thermal heating of metal
- Explosion of metal wires
- Plucked the metal atoms from the walls of the GDT

1. V.M. Batenin, V. V. Buchanov, A. M. Boichenko and etc. High-brightness Metal Vapour Lasers. Vol. 1, pp 22-62. 2017. ISBN 9781482250046

Experimental testing of induction heater

Heated samples. From left to right:

1) a twisted horizontal spiral of copper bus in a ceramic body;

2) a copper rod standing upright in a ceramic body;

3) graphite sample with a copper rod inside.

Experimental results with power consumed by induction heater of 1 kW

Sample	Theoretical Efficiency	T,°C	Heating time, s
1	≈16%	1085	180
2	≈1,5%	<400	>300
3	≈73%	1085	45

You can watch the graphite sample heating video by scanning the QR code. Or you can copy the link on the appendix slide.

Sample 1

Sample 2

Sample 3

High-speed imaging

Active optical systems

Requirements:

- selectivity, homogeneity, high G;

Advantages:

- Amplifier simultaneously highlights the object, filters and enhances the image;
- no light effect.

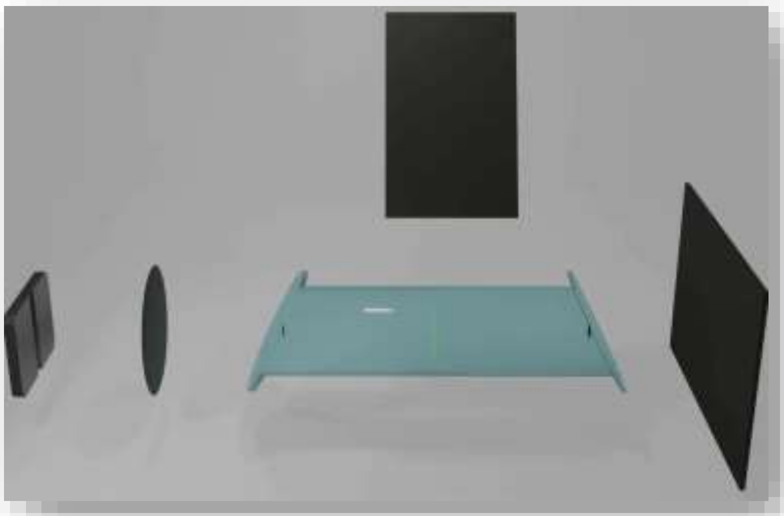

1. Within a single pulse, amplified spontaneous emission (ASE) forms the input signal of the BA and forms the background on the enhanced image.
2. The input signal includes technical noise (“parasitic” reflections from the optical elements of the circuit) and a useful signal, background radiation, and a useful signal.
3. BA operates in single-pass mode.
4. The field of view is determined by the GDT parameters, the gain profile, and the optical design.

*Brightness amplifier (BA) – the term used in the works of the group G.G. Petrash.

- High single pass gain: 10–100 dB/m
- High pulse repetition rate: 5–700 kHz
- Operates in the VIS-NIR spectrum range (510,6; 578,2 nm) - Cu
  (534,2; 542; nm), (1,29; 1,329; 1,362 um) - Mn
- Short pulse: 100 – 20 ns
- High spectral brightness

Active elements for BA

GDT parameters:

1. GL-206G: diameter 1.4 cm, length 34 cm;   Ppump 1.5 kW, P = 5 W.
2. 2. GL-201D: diameter 2 cm, length 123 cm; Ppump 3.5 kW, P = 40 W

Frequency not more than 16 kHz, access to the mode up to 1 h, dependence of the mode on the pump parameters

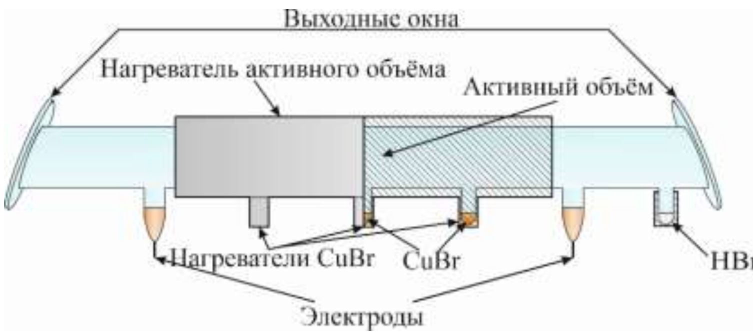

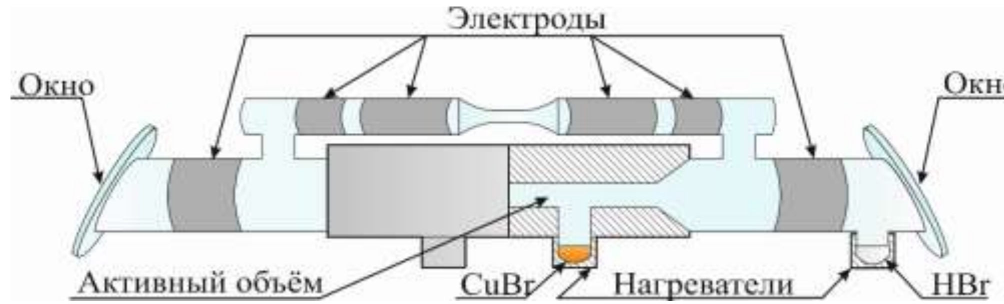

System with independent heating (CuBr-AT - laser)

- allows to change the temperature parameters of the active element without changing the excitation parameters

Excitation method (capacitive GDT)

- tehere is no contact with the active medium of the element, which simplifies manufacturing and increases the service life.

Power supplies with a pulsed charge of working capacitor

- long life-time, low weight and size parameters

Power supplies based on tacitrons

- possibility of increasing the FRR without special means, large specific energy inputs

Active optical systems

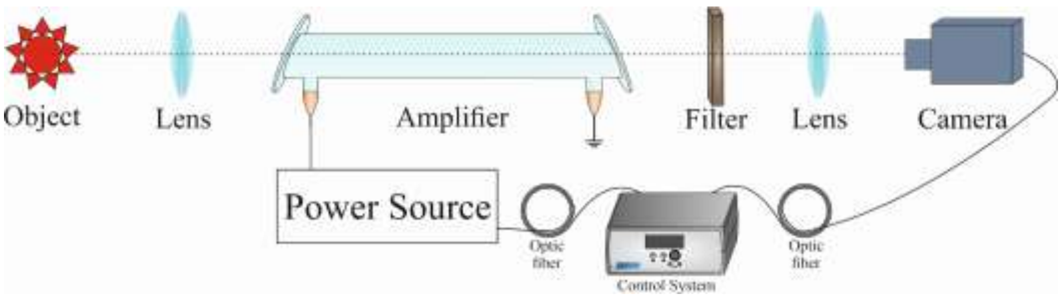

!It needs!

- High intensity lasers
- Visible range of the spectrum
- Short pulse duration
- Fast shutter of the camera

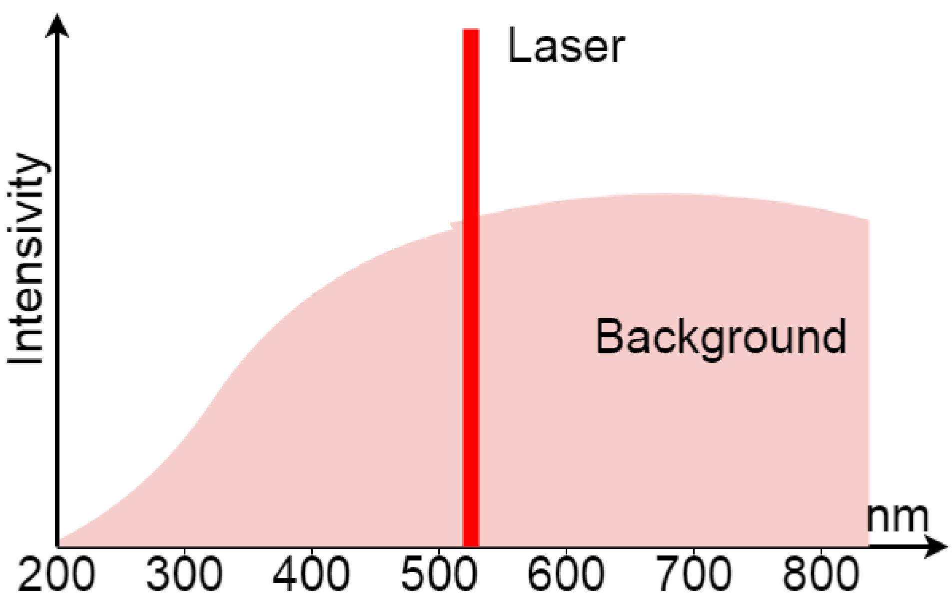

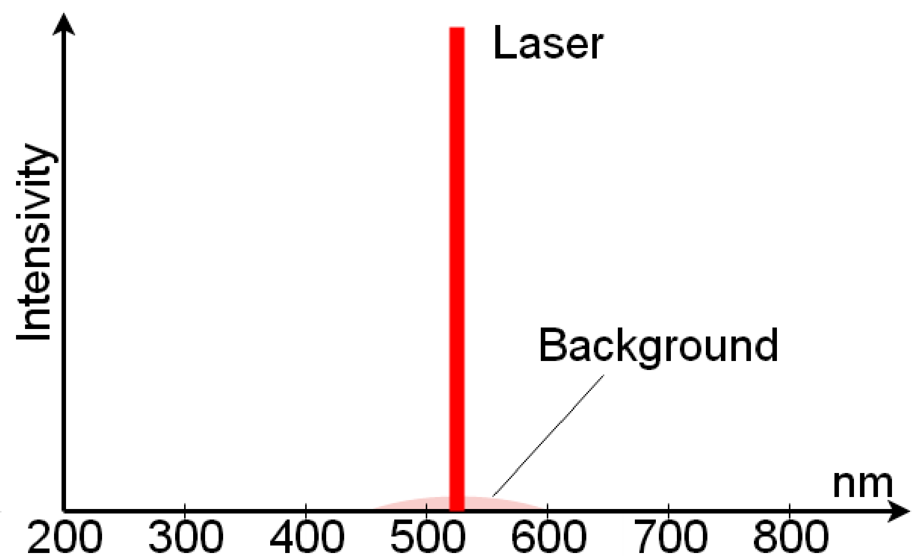

The optical signal processing by the active optical system

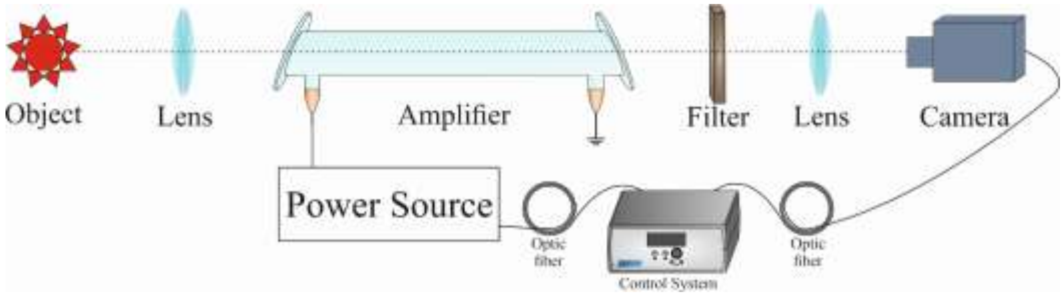

!It needs!

- High intensity lasers
- Visible range of the spectrum
- Short pulse duration
- Fast shutter of the camera

Temporal + Spectral Filtration

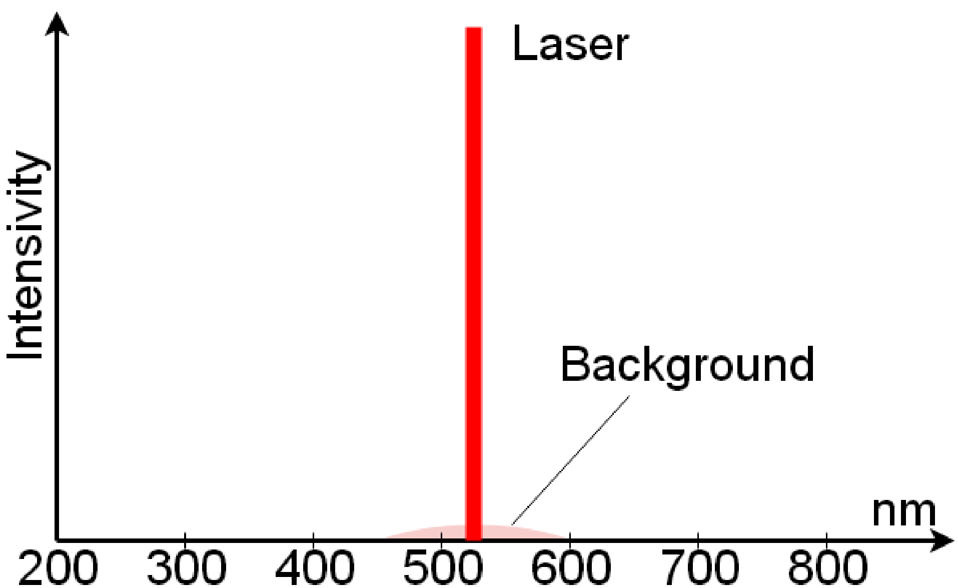

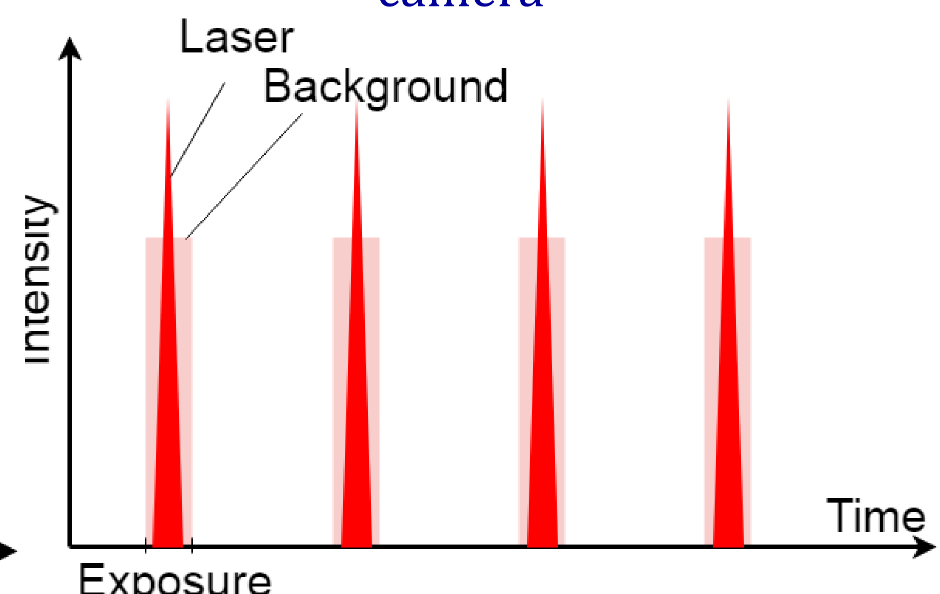

Metal halide active medium for high-speed imaging

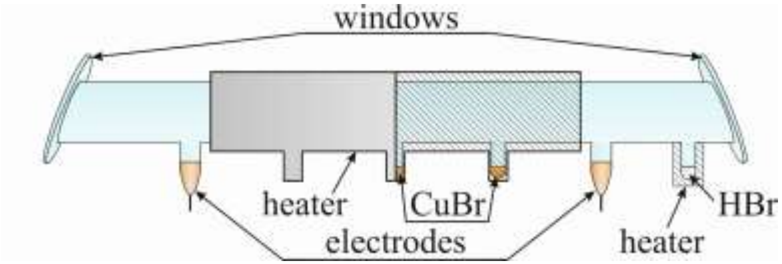

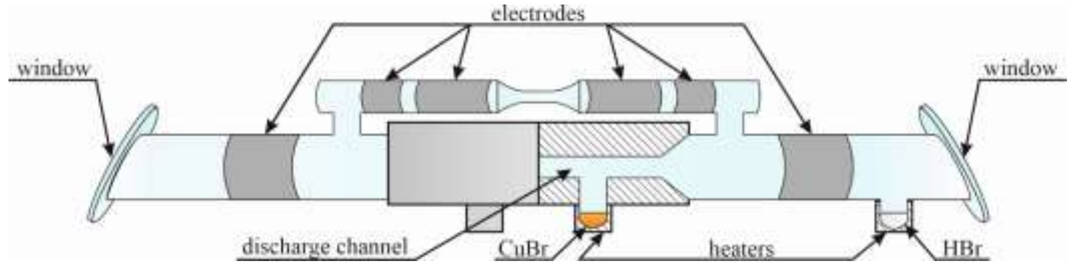

Advantages

- High gain: 10–100 dB/m (0.2 cm^{-1})
- High pulse repetition rate: 5–700 kHz
- Visible and near IR range of the spectrum

(510.6 & 578.2 nm) , (534,2; 542 nm),

(1,29; 1,329; 1,362 um)

- Laser pulse width: 20 – 100 ns
- High spectral brightness

Abilities

- ASE mode
- High time resolution
- Using modern imaging equipment
- Low distortion
- High level of signal filtering

High-speed BA on copper atom transitions

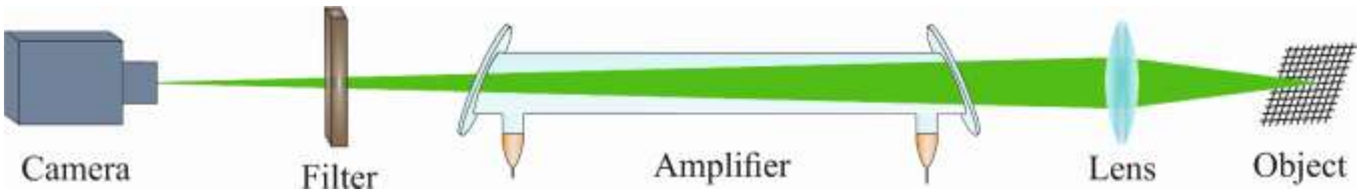

Laser Monitor Scheme

CuBr,
Typical pumping
λ_1= 510,6 nm,
Ø 25 mm, L = 500 mm
P = 1200 W

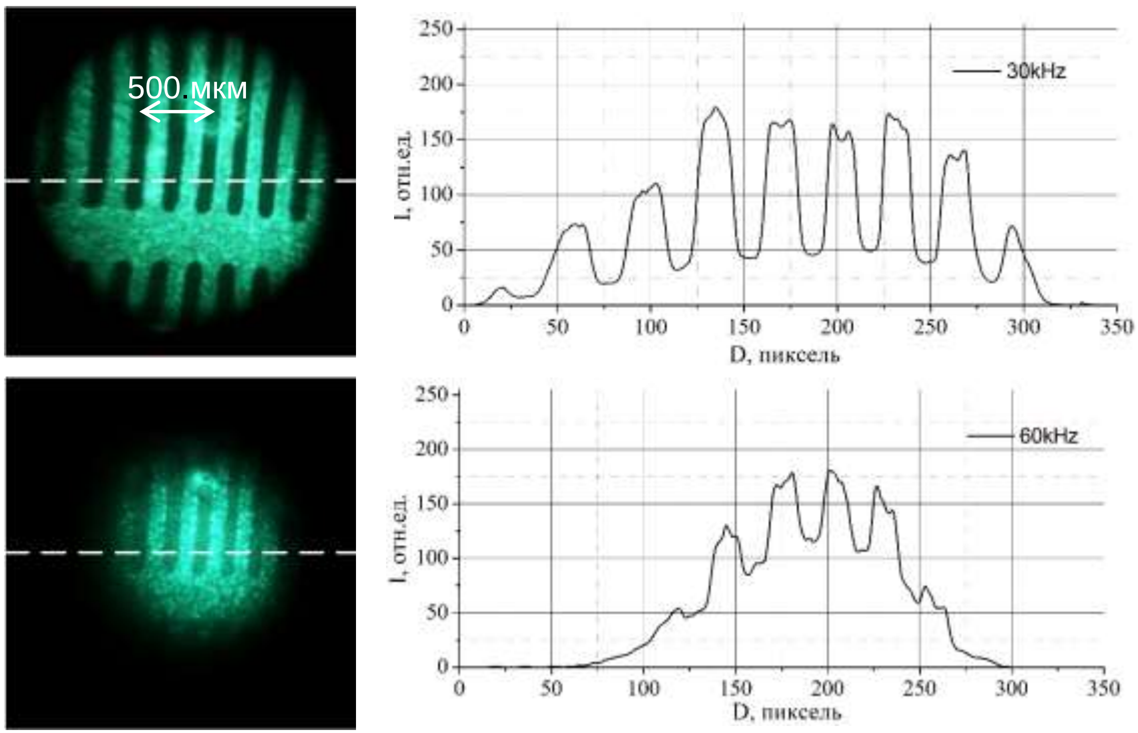

The results of visualization of a metal mesh in a laser monitor with different PFR excitation

For the development of high-frequency BAs, it is necessary to use special solutions that would make it possible to create laser monitors on their basis.

Optimization BA operating mode. Effect of HBr additive

CuBr, traditional GDT

GDT Ø 50 mm, L = 900 mm

PRF – 30 kHz,

E = 108 mkJ/cm^3

(*) Modification of process kinetics due to HBr:

- work at high PRF;
- increase the effective diameter of the beam;
- improve generation characteristics.

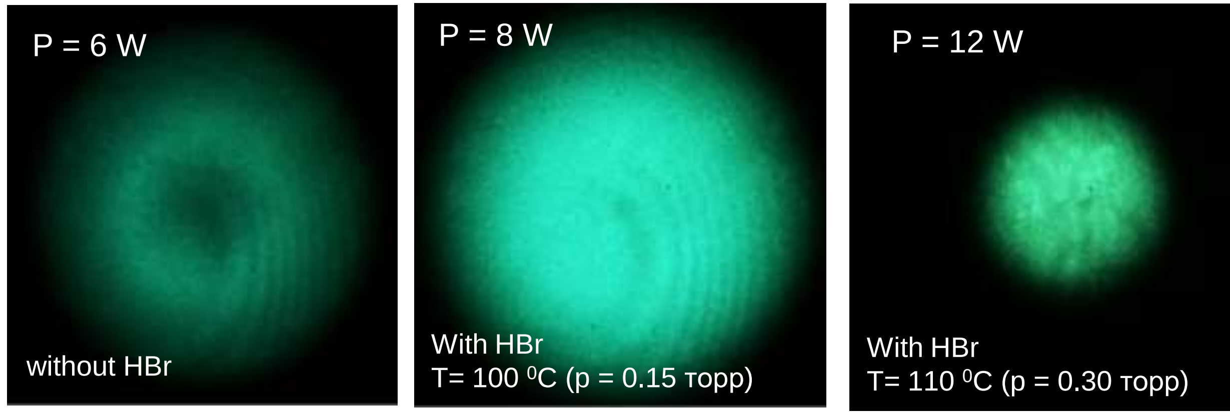

Images of a single-pass radiation pulse at various concentrations of HBr

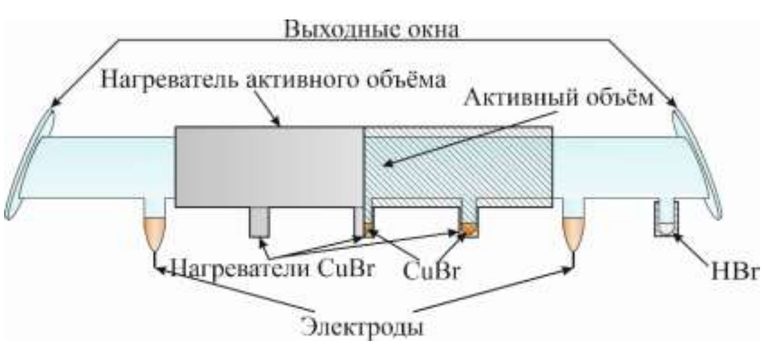

The construction provides:

1. Stabilized GDT temperature
2. Independently changing of CuBr и HBr

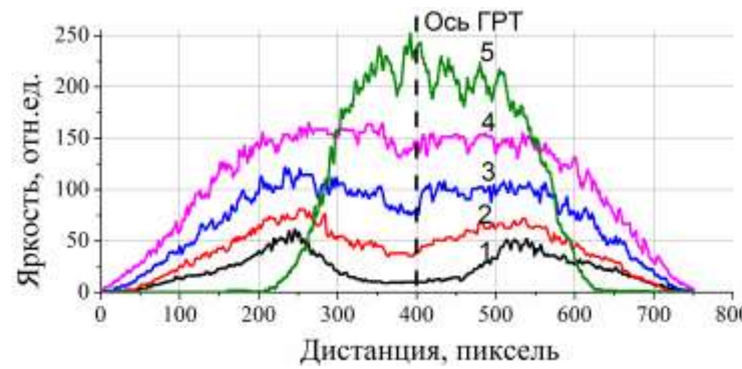

Профиль однопроходного излучения при различной концентрации HBr в активной среде

1 – without HBr;

2, 3 – increasing of HBr 100 ^{0}C;

4 – stabilized concentration of HBr 100 ^{0}C;

5 – stabilized concentration of HBr 110 ^{0}C.

1. Шиянов Д.В. Лазер на парах бромида меди с высокой частотой следования импульсов. Дисс… к.ф.-м.н. Томск. – 2007. (ИОА СО РАН).

2. Gubarev F.A., Trigub M.V., Klenovsky M.S., Lin L, Evtushenko G.S. Radial distribution of radiation in a CuBr vapor brightness amplifier used in laser monitors // Applied Physics B - Lasers and Optics. 2016. V. 122. Iss. 1. Article number 2. P. 1–7.

Optimization BA operating mode. Effect of CuBr concentration

CuBr, typical GDT

ГРТ Ø 50 mm, L = 900 mm

PRF – 30 kHz,

E = 108 mkJ/cm^3

(*)Amplification features tuning:

- High PRF operating mode;
- Increasing diameter amplification profile;
- Improving lasing features.

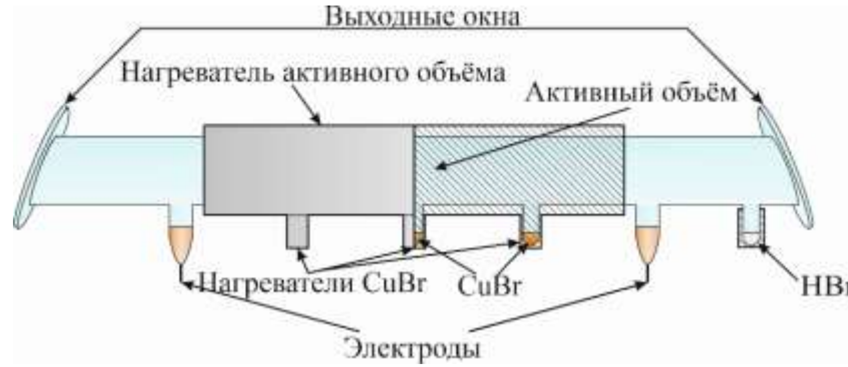

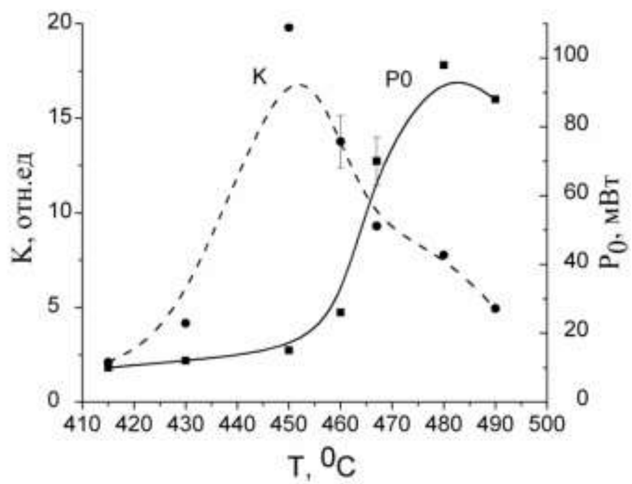

Dependence of single-pass gain (K) and ASE power (P0) on CuBr concentration.

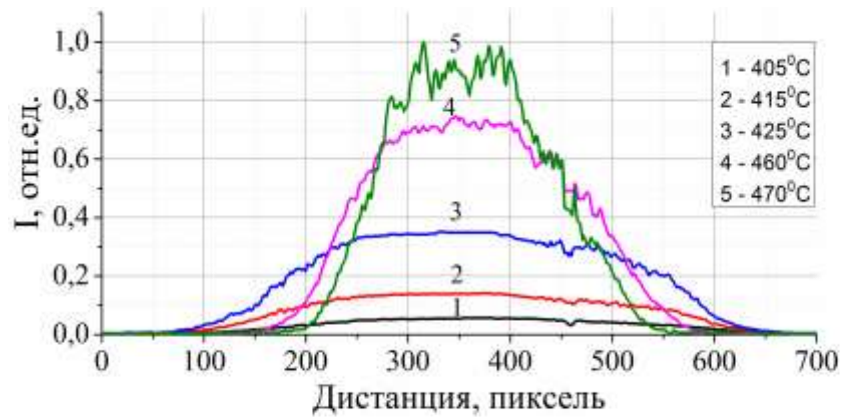

Single pass gain profile versus CuBr concentration.

1. Evtushenko, G.S., Torgaev S.N., Trigub M.V., Shiyanov, D.V., Evtushenko T.G., Kulagin, A.E. High-speed CuBr brightness amplifier beam profile // Optics Communications. 2017. V. 383. P. 148–152.

2. Кулагин А.Е., Торгаев С.Н., Евтушенко Г.С., Тригуб М.В. Кинетика активной среды усилителя яркости на парах меди // Известия вузов. Физика. 2017. Т. 60. № 11. С. 122–127.

Optimization BA operating mode. Effect of CuBr concentration

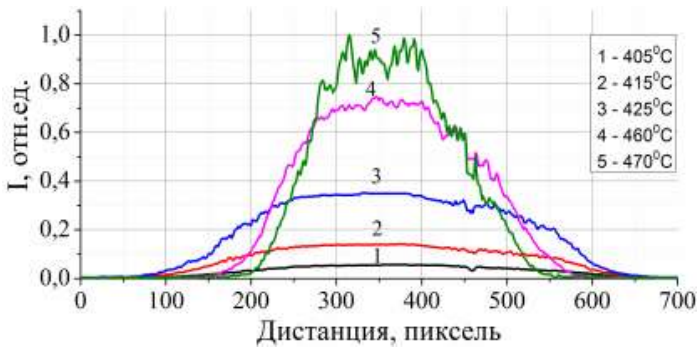

Single-pass gain profile versus CuBr concentration.

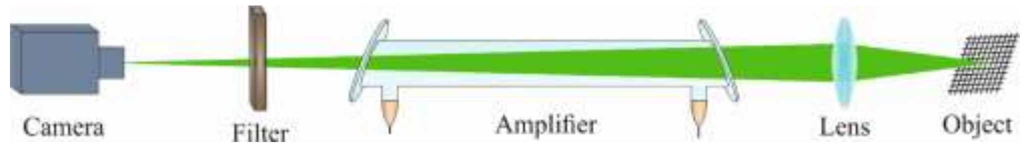

415⁰C

430⁰C

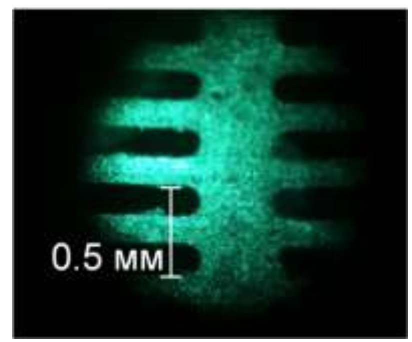

450⁰C

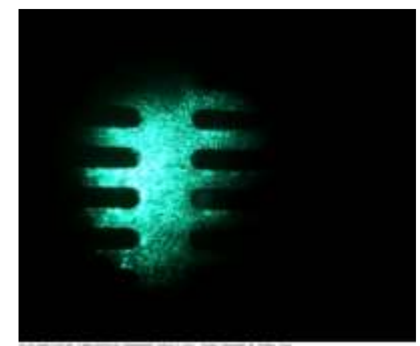

460⁰C

Metal grid imaging results at different CuBr concentrations

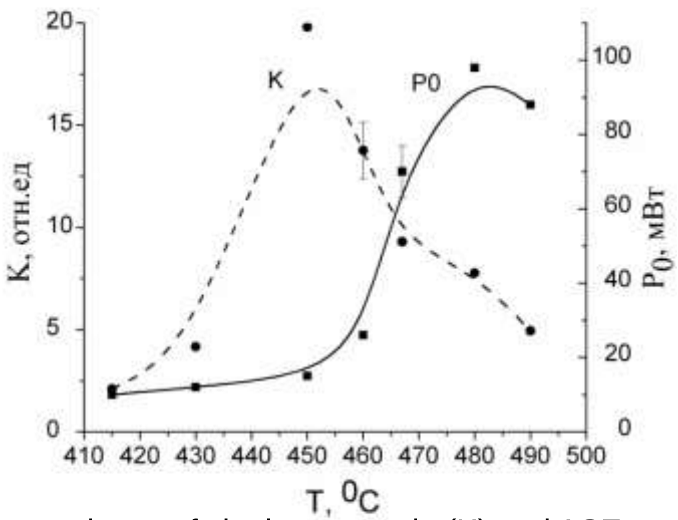

Dependence of single-pass gain (K) and ASE power (P0) on CuBr concentration.

1. Evtushenko, G.S., Torgaev S.N., Trigub M.V., Shiyanov, D.V., Evtushenko T.G., Kulagin, A.E. High-speed CuBr brightness amplifier beam profile // Optics Communications. 2017. V. 383. P. 148–152.
2. Кулагин А.Е., Торгаев С.Н., Евтушенко Г.С., Тригуб М.В. Кинетика активной среды усилителя яркости на парах меди // Известия вузов. Физика. 2017. Т. 60. № 11. С. 122–127.

High-speed BA on copper atom transitions

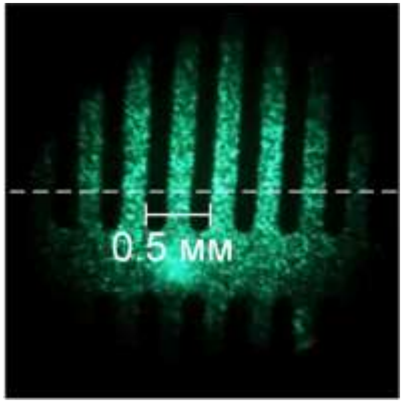

60 kHz

70 kHz

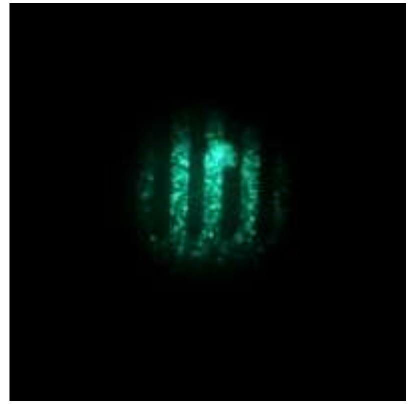

80 kHz

CuBr,
Typical GDT
Ø 25 mm, L = 500 mm
modulator –TGU1-1000/25

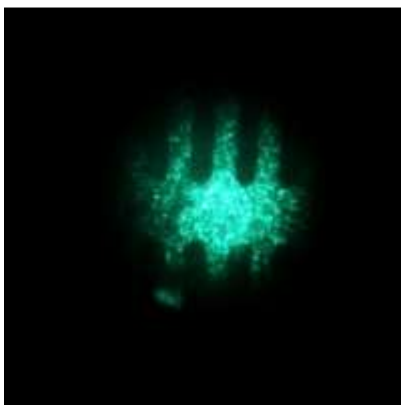

90 kHz

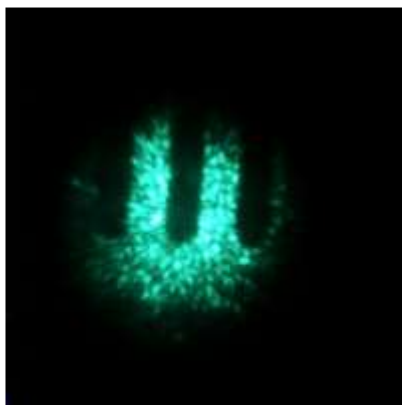

100 kHz

Images of the test object at different PRF.

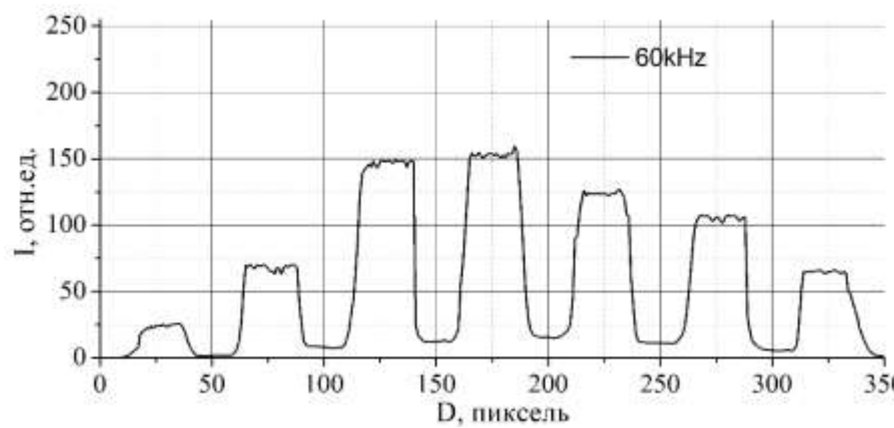

Pixel intensity distribution at 60 kHz PRF.

1. Тригуб М.В., Шиянов Д.В., Суханов В.Б., Евтушенко Г.С. Активная среда на парах бромида марганца с внутренним реактором при частоте следования импульсов до 100 кГц // Оптика атмосферы и океана. 2014. Т.27. № 4. С. 321–325.
2. Trigub M.V., Evtushenko G.S., Torgaev S.N., Shiyanov D.V., Evtushenko T.G. Copper bromide vapor brightness amplifiers with 100 kHz pulse repetition frequency // Optics Communications. 2016. V. 376. P. 81–85.

High-speed BA on manganese atom transitions

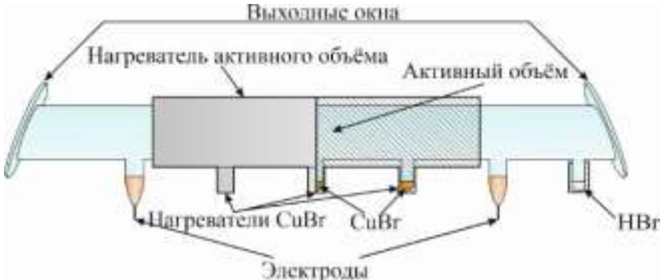

$MnCl_2$, typical GDT

GDT Ø 10 mm, L = 300 mm

PRF – 17 kHz, E = 850 mkJ/cm^3

PRF – 100 kHz, E= 150 mkJ/cm^3

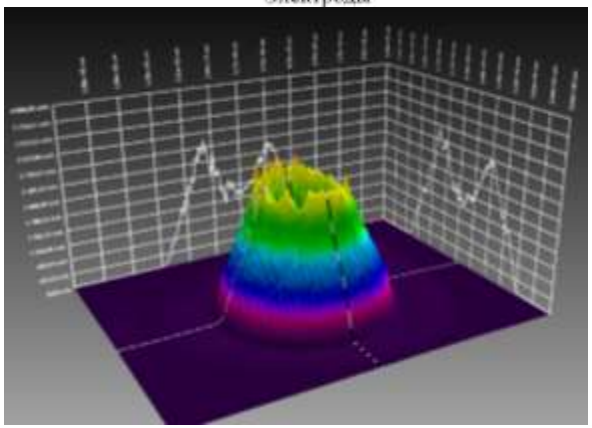

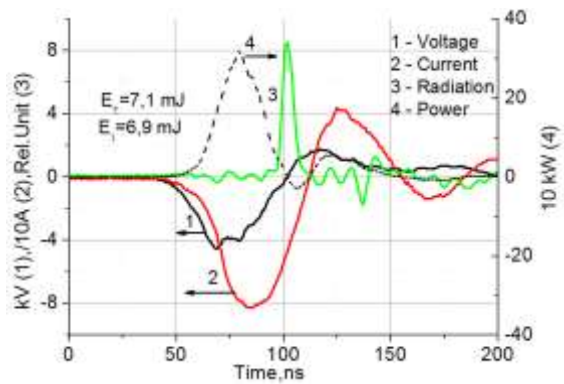

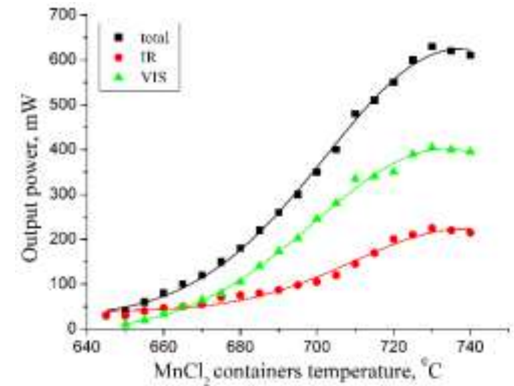

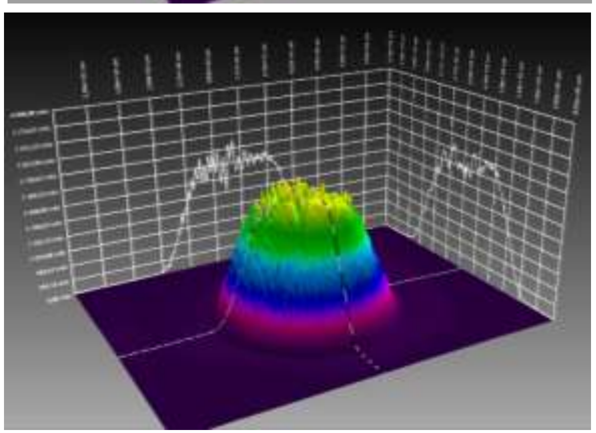

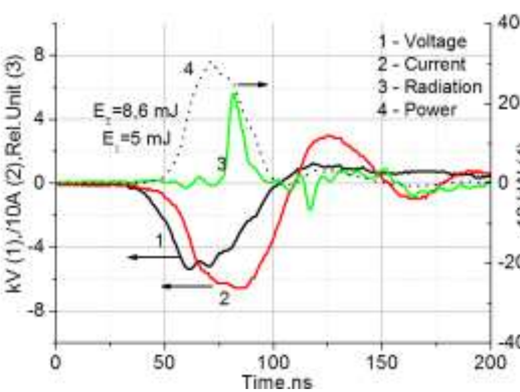

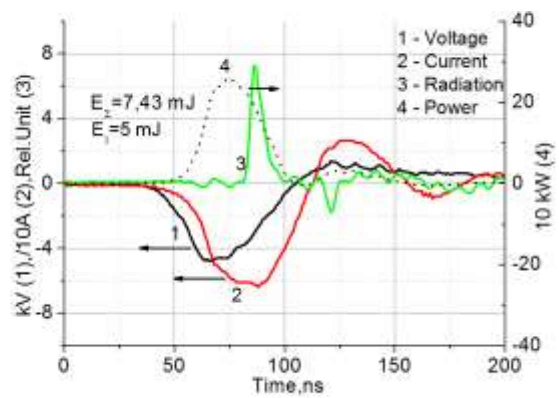

1.Тригуб М.В., Шиянов Д.В., Суханов В.Б., Петухов Т.Д., Евтушенко Г.С. Усилитель яркости на переходах атома марганца с частотой следования импульсов до 100 кГц // Письма в ЖТФ. 2018. Т. 44. Вып. 24. С. 135–142.

2. Shiyanov D.V., Trigub M.V., Sokovikov V.G., Evtushenko G.S. MnCl2 laser with pulse repetition frequency up to 125 kHz // Optics and Laser Technology. 2020. V. 129. DOI: 10.1016/j.optlastec.2020.106302.

VIS-NIR BA for laser monitors

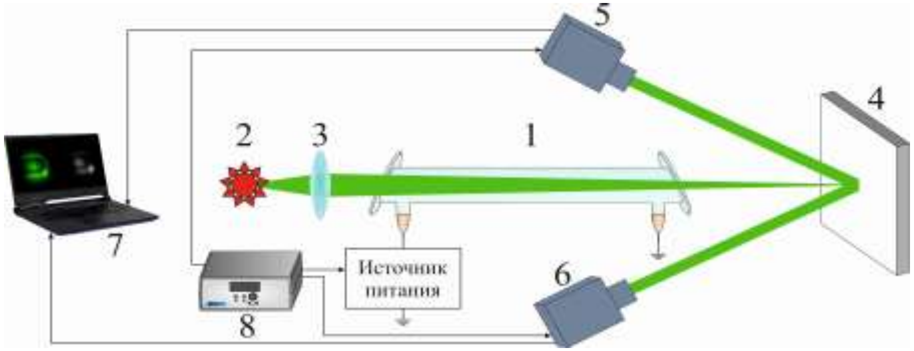

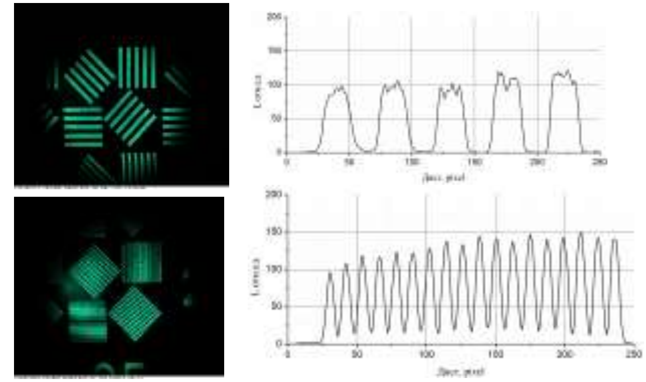

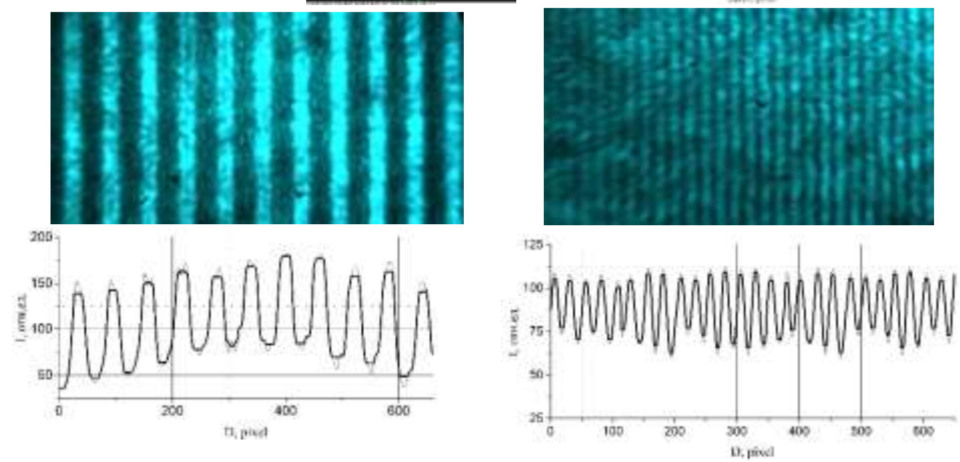

CuBr, typical GDT

GDT Ø 16 mm, L = 200 mm

PRF – 100 kHz, E = 104 mkJ/cm^3

camera: MegaSpeed MS103

MnCl2, typical GDT

GDT Ø 10 mm, L = 300 mm

PRF – 17 kHz, E = 850 mkJ/cm^3

PRF – 100 kHz, E= 150 mkJ/cm^3

Camera: MegaSpeed MS103,
SWIR NPO «ORION»

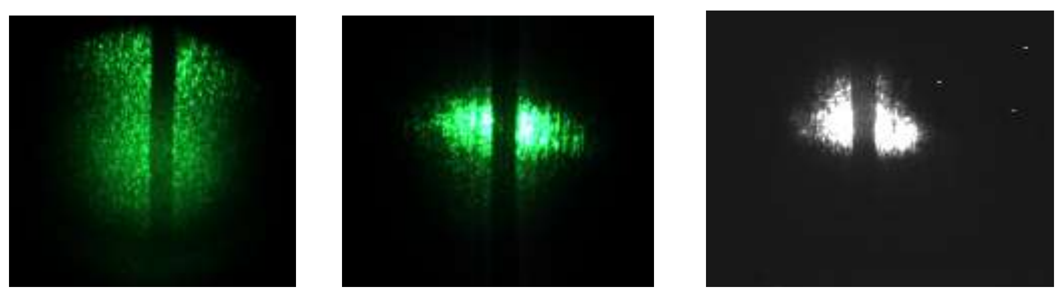

1. Evtushenko G.S., Trigub M.V., Gubarev F.A., Evtushenko T.G., Torgaev S.N., Shiyanov D.V. Laser monitor for non-destructive testing of materials and processes shielded by intensive background lighting, Review of Scientific Instruments. – 2014. – Vol. 85. – Iss. 3. – № 033111. – Pp. 1-5.

SHS visualization using the laser illumination method

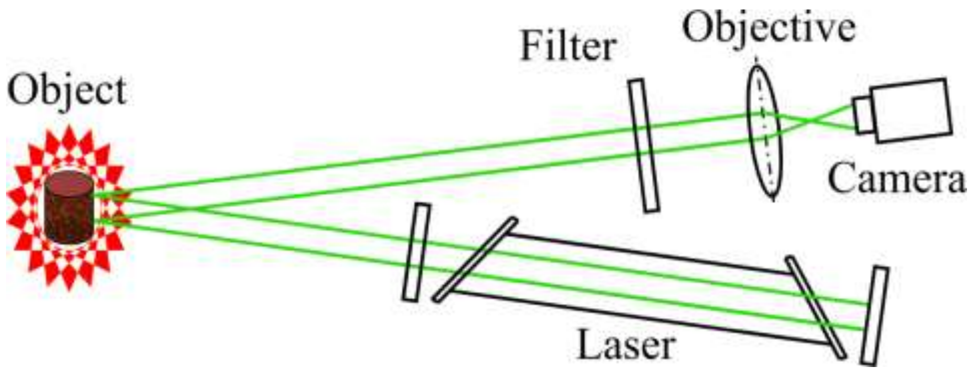

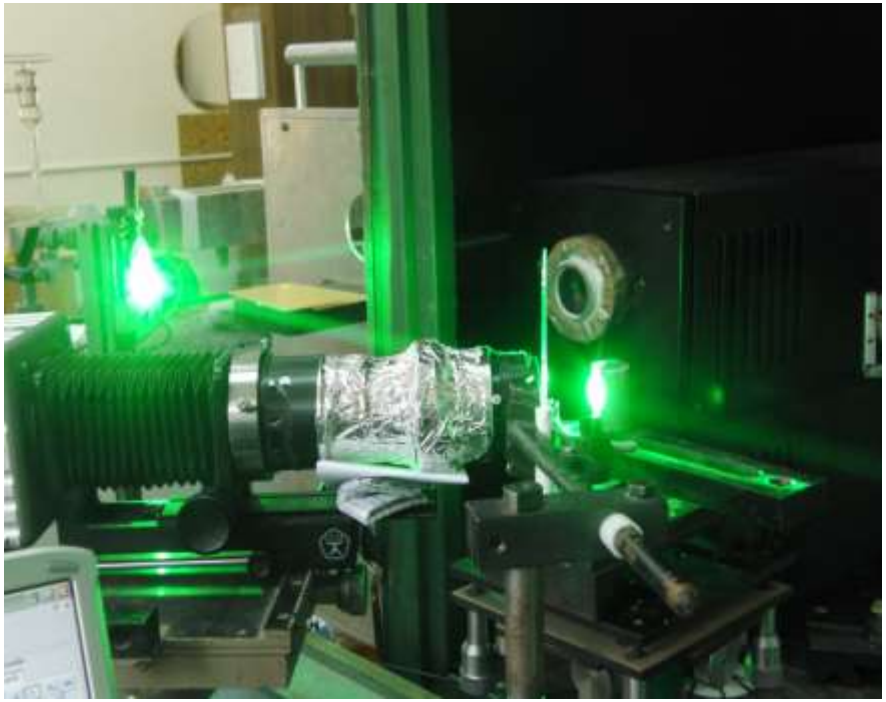

Field of view – 5 mm.
Shooting speed – 1400 frames/sec.
Camera – MotionPro X3
Frame-by-frame imaging
Radiation power– 2.5 W

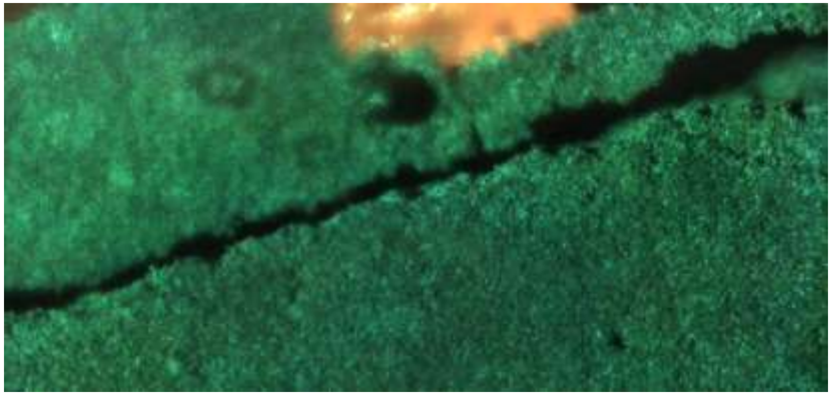

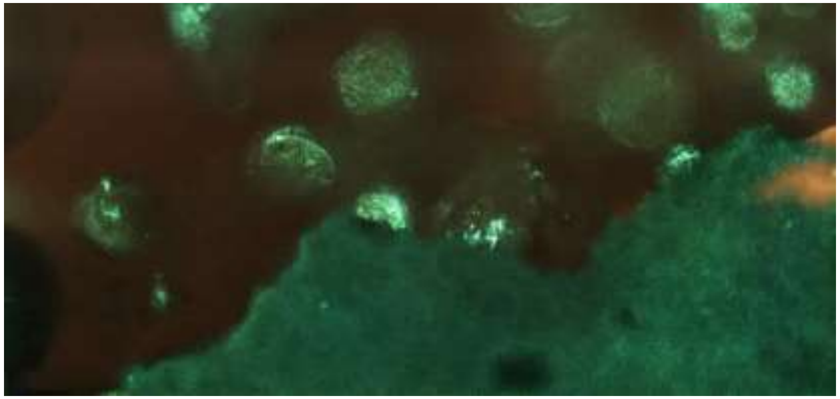

Ni + 25%Al+ 0.2%$CaCO_3$

SHS imaging with the CuBr active element

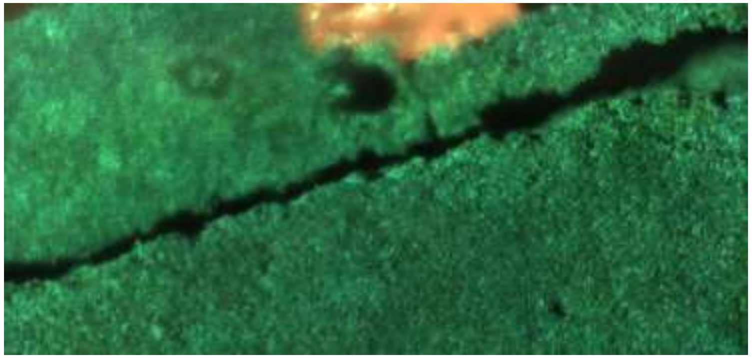

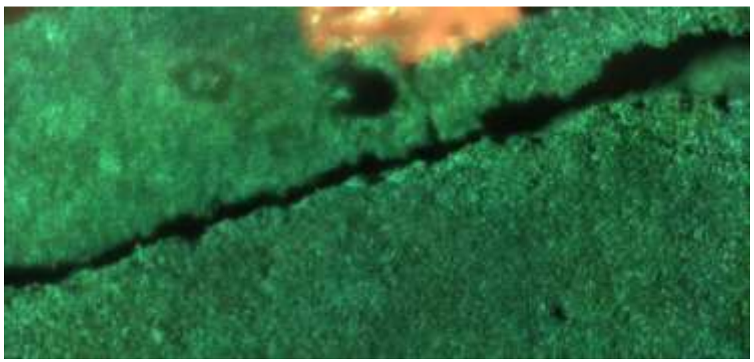

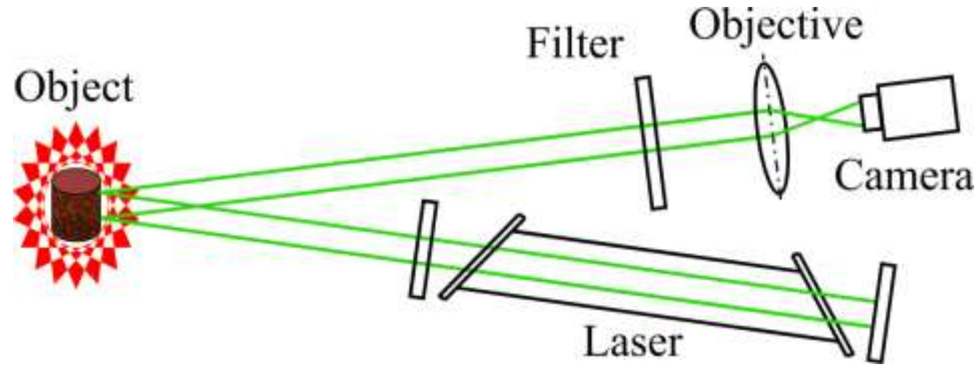

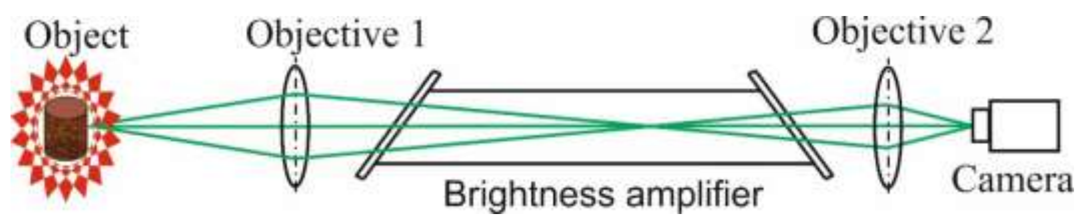

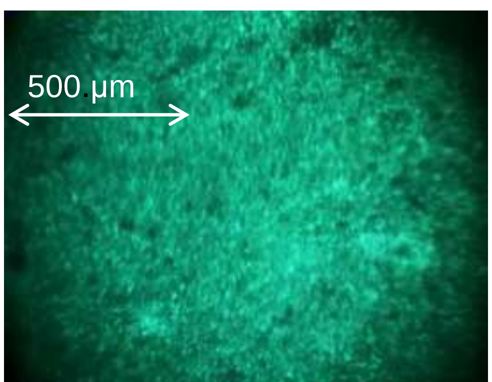

TiO_3 + 55%Al

(65%$FeTiO_3$ + 35%Al) + 35% kaoline

Field of view – 1.5 mm
Shooting speed – 2400 frames/sec.
Camera – Fastec HiSpec 1

SHS imaging with the laser monitor

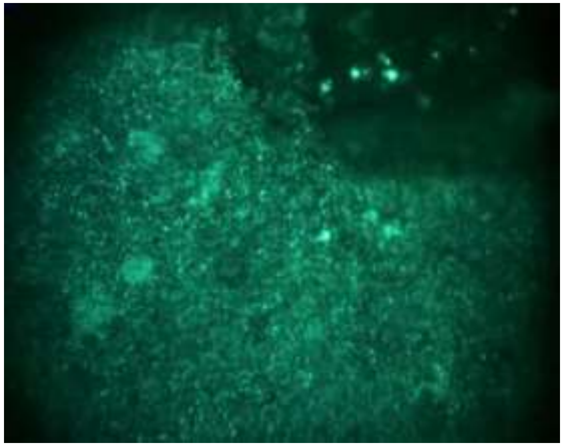

(65%$FeTiO_3$ + 35%Al) + 35% kaoline

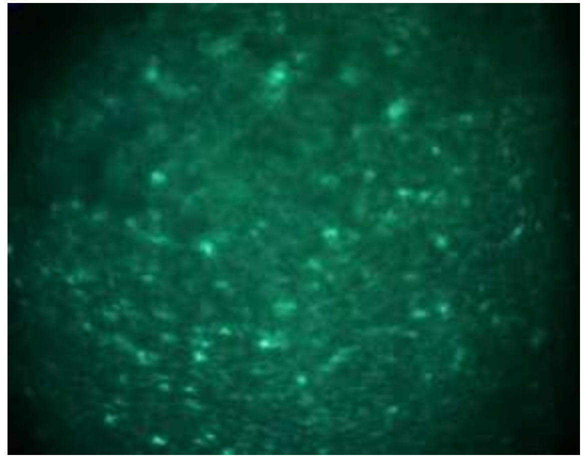

80%Ni + 20%Al

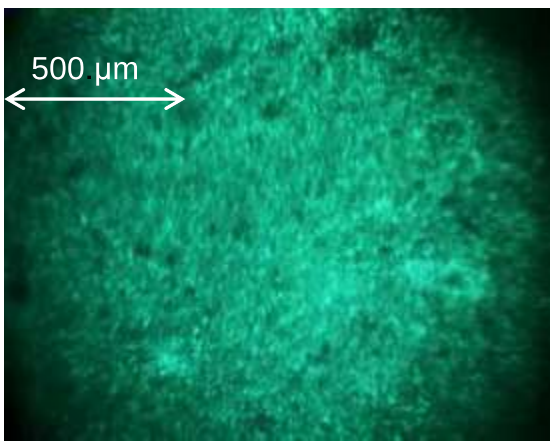

TiO_3 + 55%Al

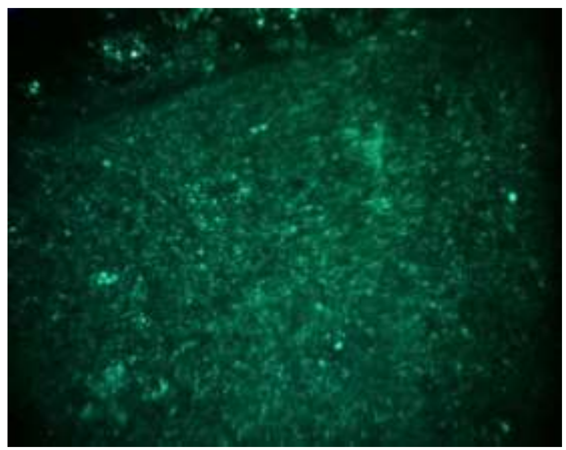

«Sayan mixture»

Field of view – 1.5 mm
Shooting speed – 2400 frames/sec.
Camera – Fastec HiSpec 1

T = ***1700 - 3000 K***

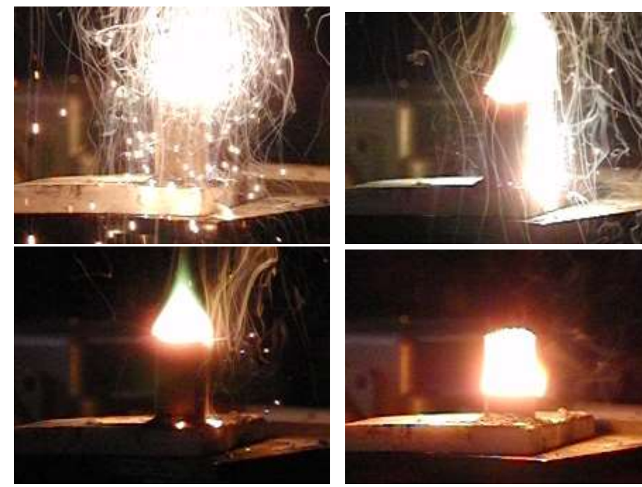

VIS-NIR BA applications

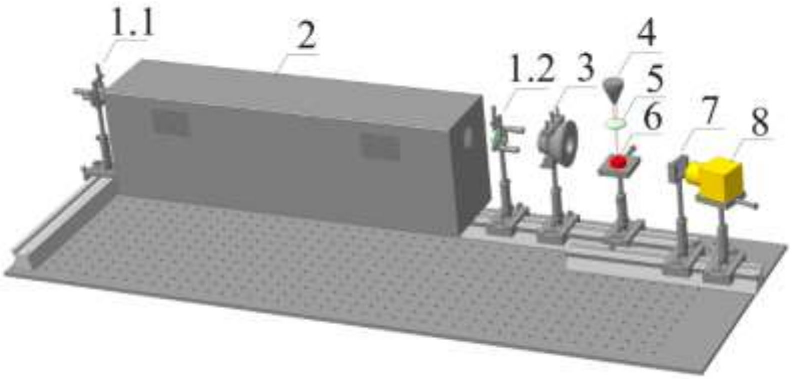

It allows to see the light diffused by nanopowder.

GDT Ø 2 cm,
L = 38 cm
F = 21.4 kHz,
Texp=3; 50 us
Frame-by-frame

Power laser:
Ytterbium fiber laser
LS-07-H, pulse mode,
Ø 400 um, 1 J

Materials:
YSZ
C
Fe2O3
Nd:Y2O3
Al2O3

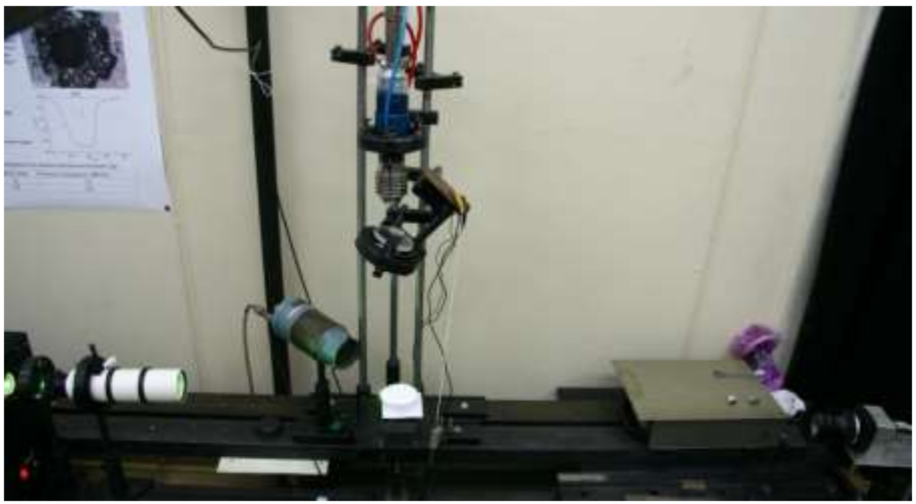

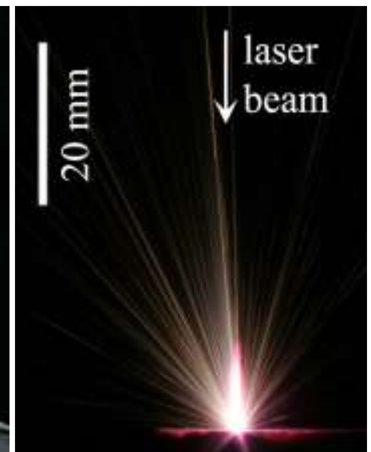

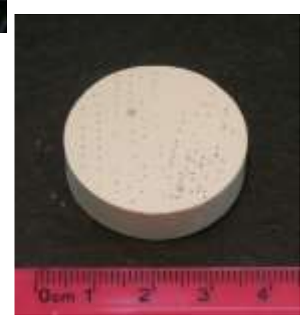

Nd:Y2O3, 50us, self-radiation

In collaboration with our colleagues from Institute of Electrophysics

VIS-NIR BA applications for illumination method realization

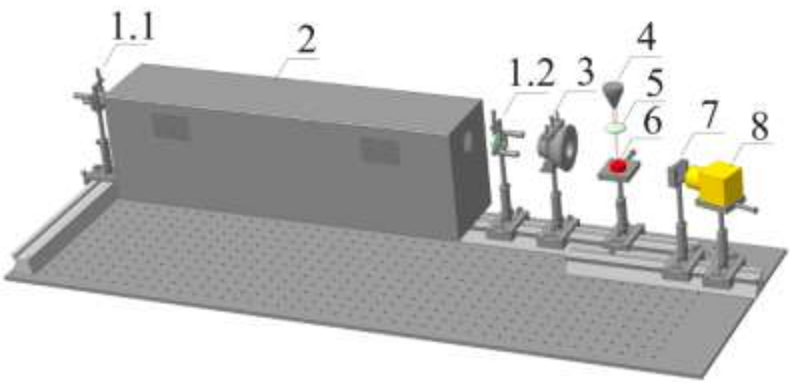

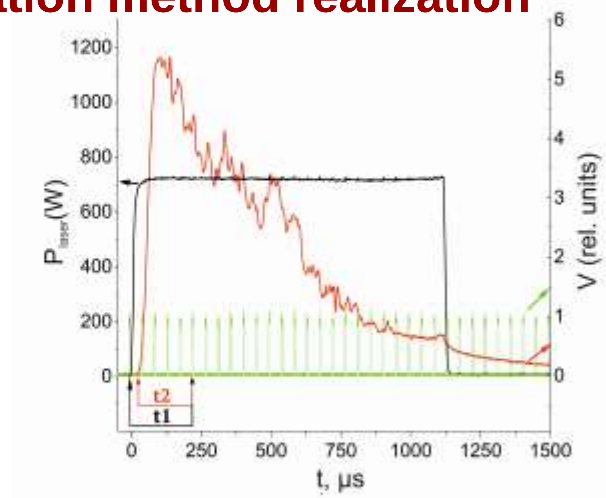

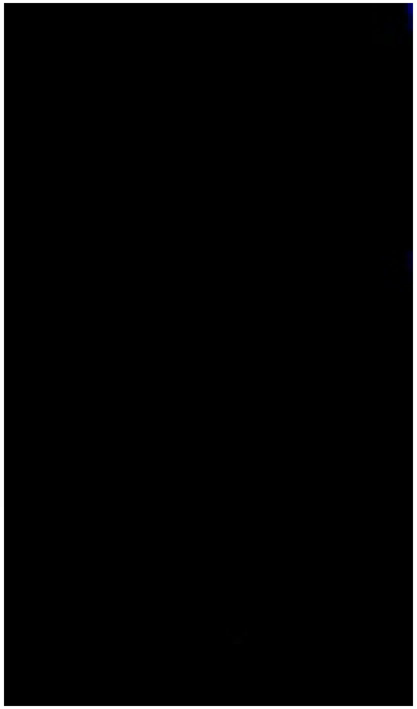

Nd:Y2O3, reflected, 3 us

F shooting = 11000 frames/sec.

Without illumination

Nd:Y2O3, reflected, 3us

F shooting = 11000 frames/sec.

Nd:Y2O3, reflected, 50us

F shooting = 11000 frames/sec.

VIS-NIR BA applications for lser monitor realizations

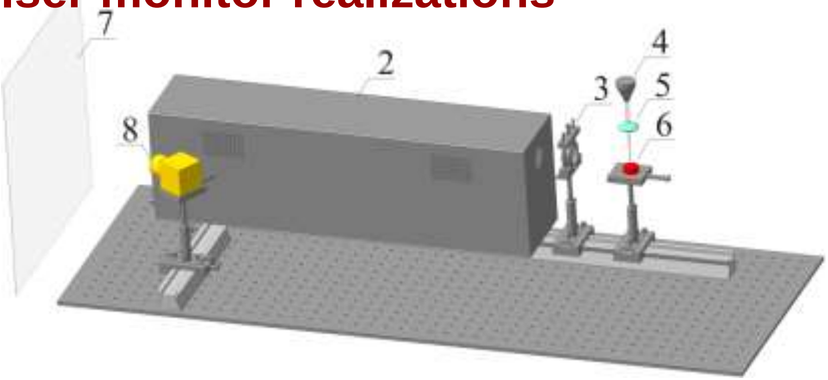

It is used for the visualization of optical inhomogeneities and "big" particles. It allows the depth filtration of an optical signal.

Nd:Y2O3, reflected, 3 μs, 250 mm

F shooting = 11000 frames/sec.

Nd:Y2O3, 3 μs, 500 mm

F shooting = 11000 frames/sec.

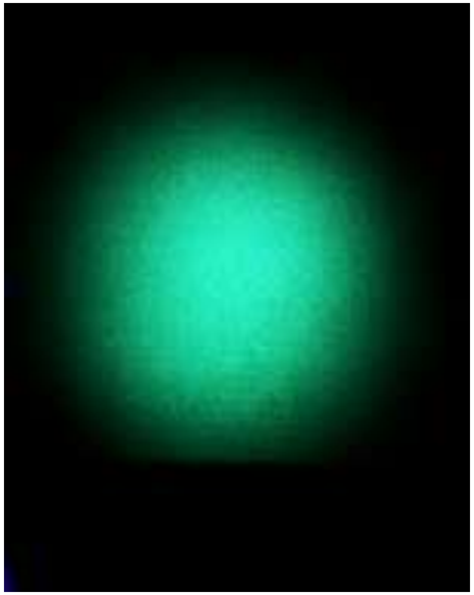

Active methods Versus Passive methods

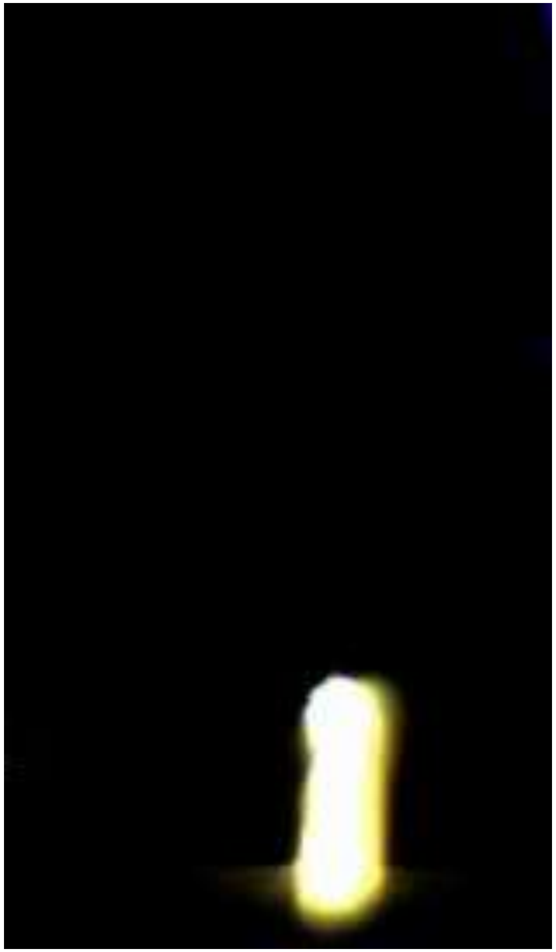

The use of both methods allows to get new information about fundamental problems!

Imaging in the laser monitor

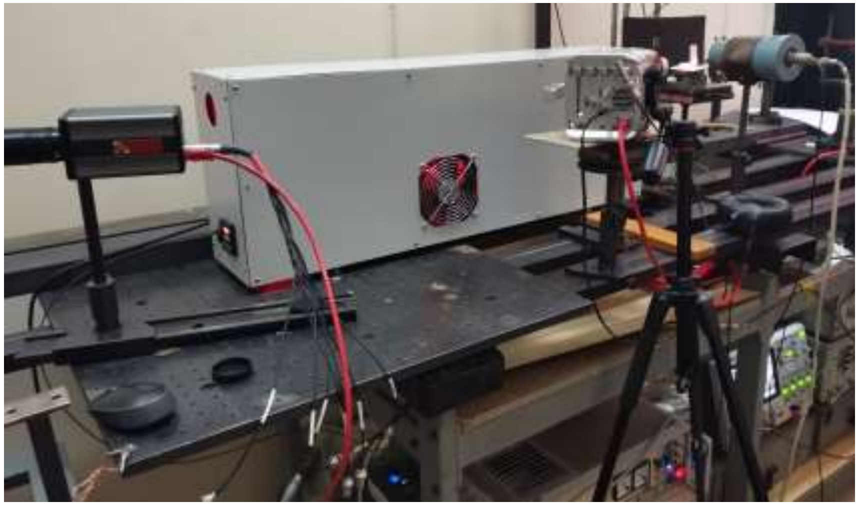

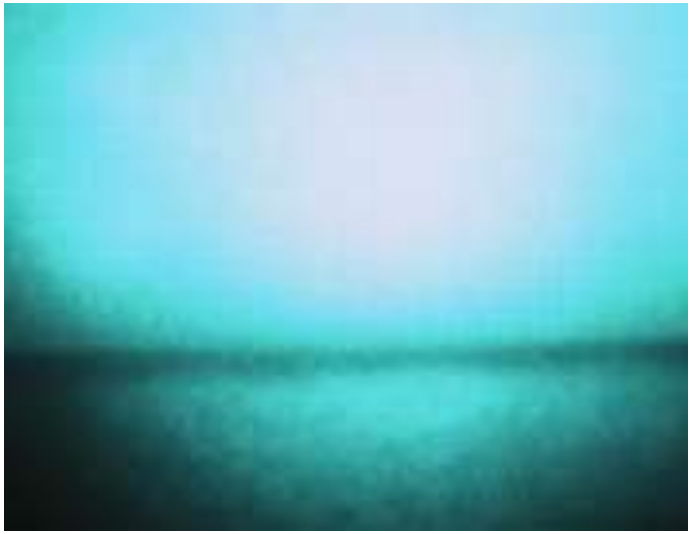

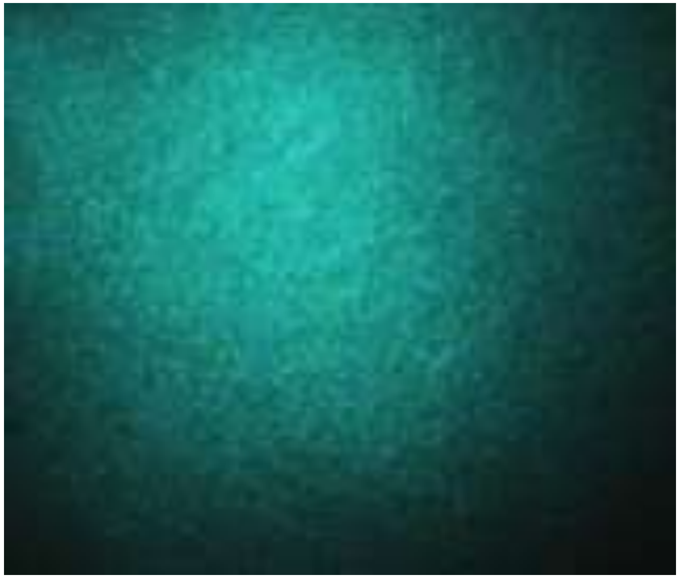

Nd:Y2O3, reflected, 2 μs, 250 mm

F shooting = 25000 framessec.

BA application in imaging methods

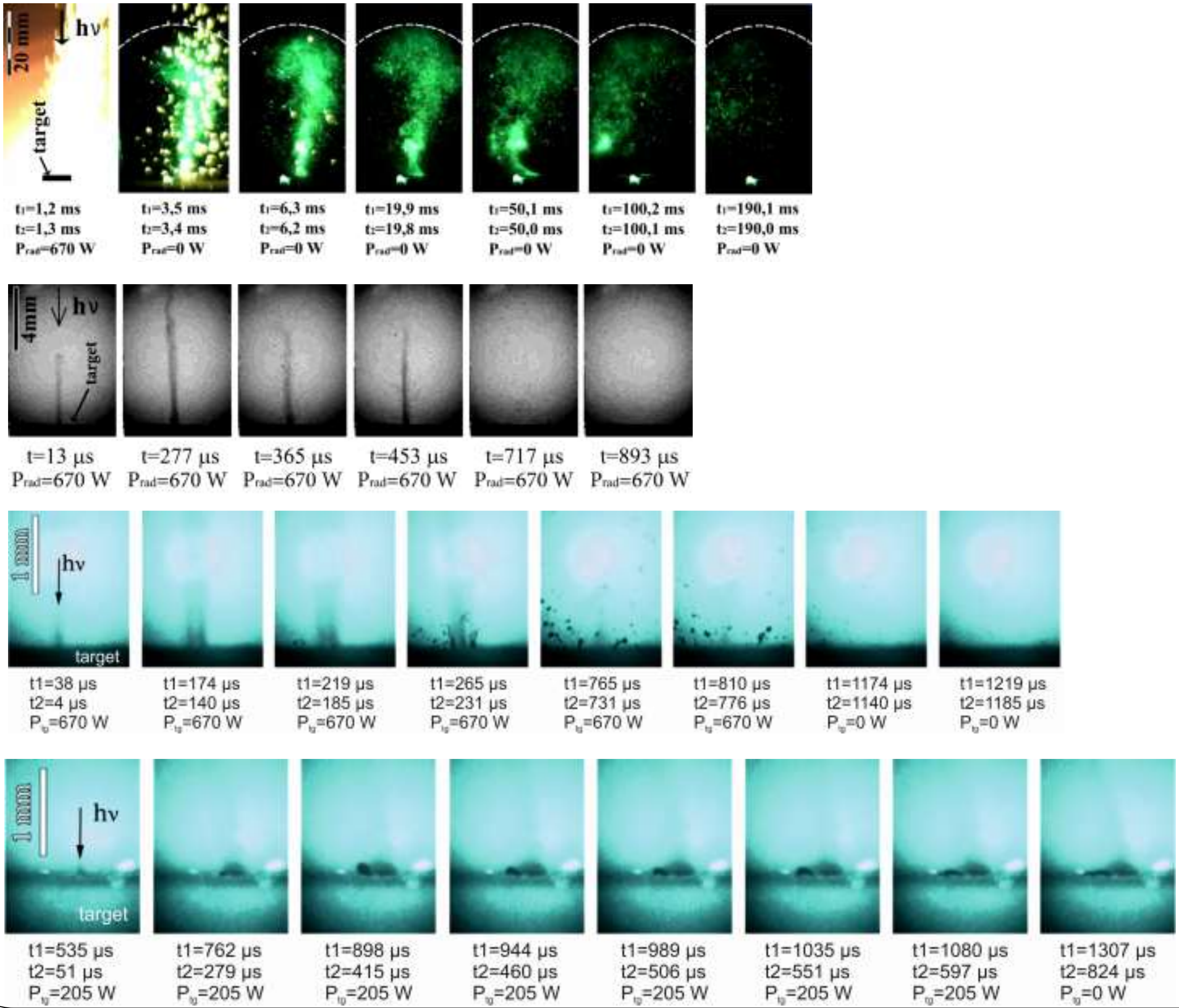

Bistatic Laser Monitor – Independent source plus BA

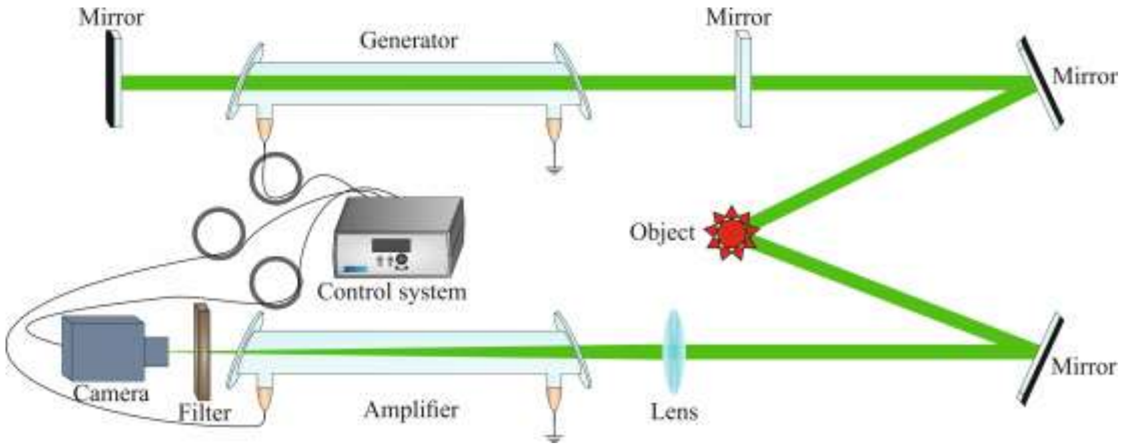

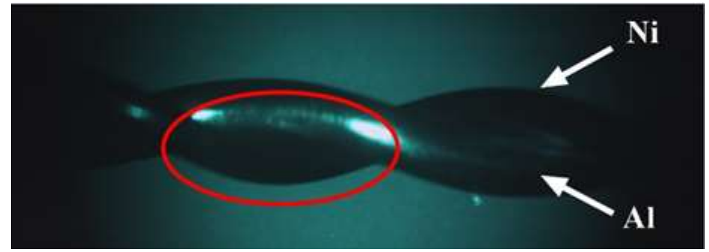

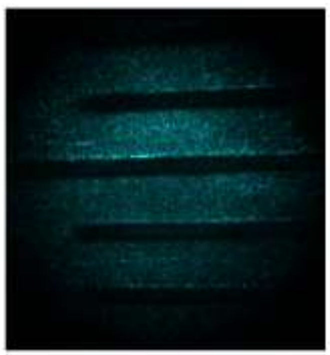

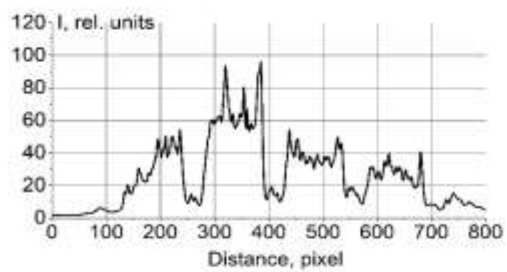

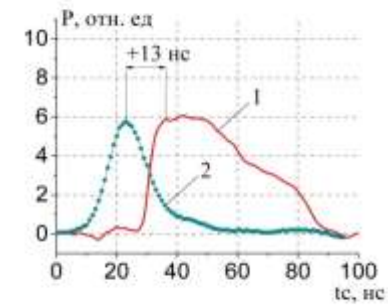

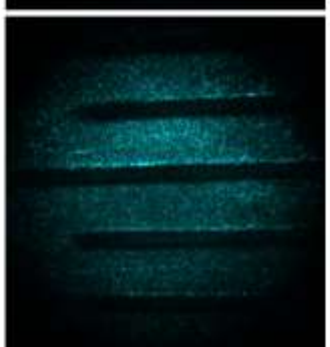

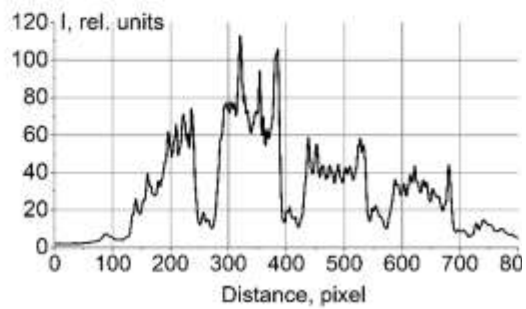

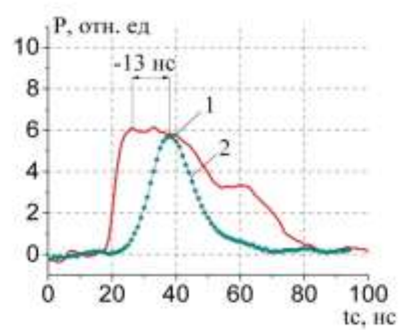

Imaging distance – 1,4 m.
Field of view is increased in 1,45 times
Local contrast increased in 2 times

Bistatic Laser Monitor – Independent source plus BA

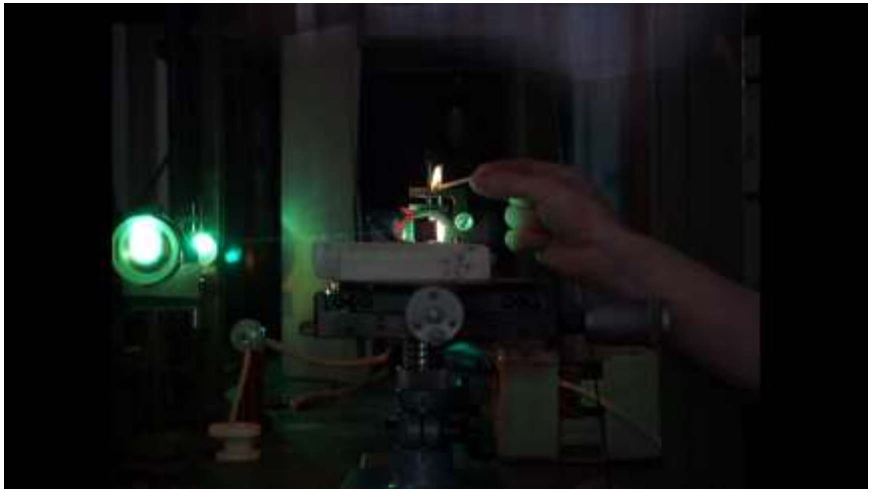

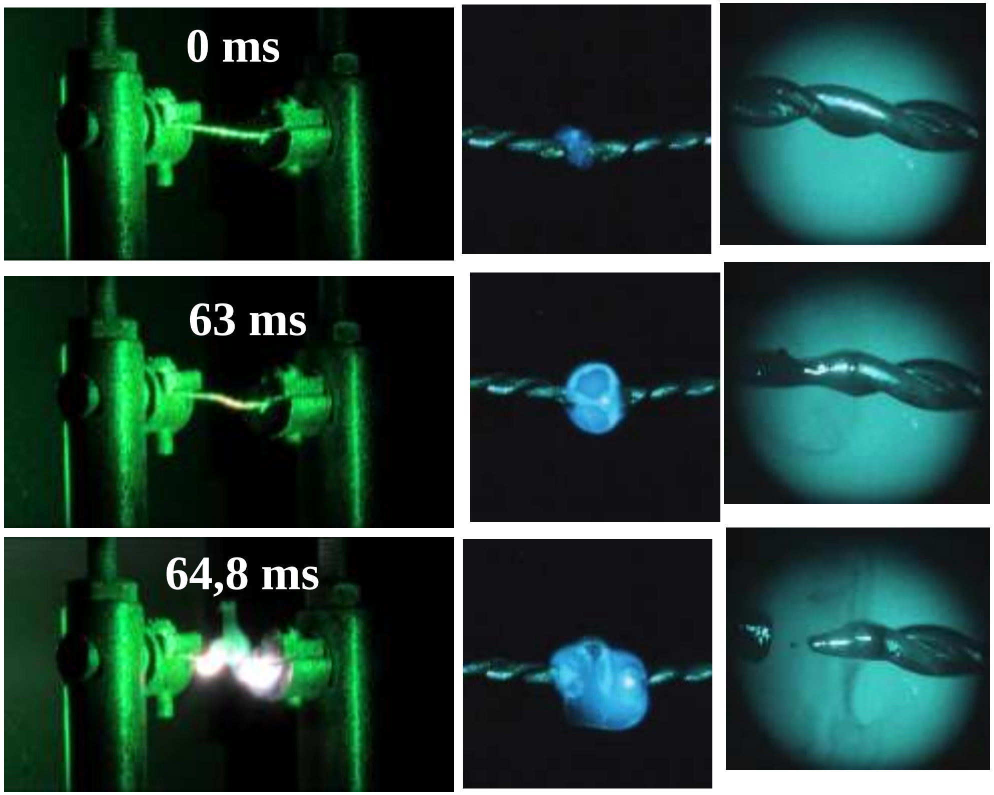

Object:
conductors (Ni) + (Al)
Frame rate: 15000 fps
Process:
Burning of Ni+Al

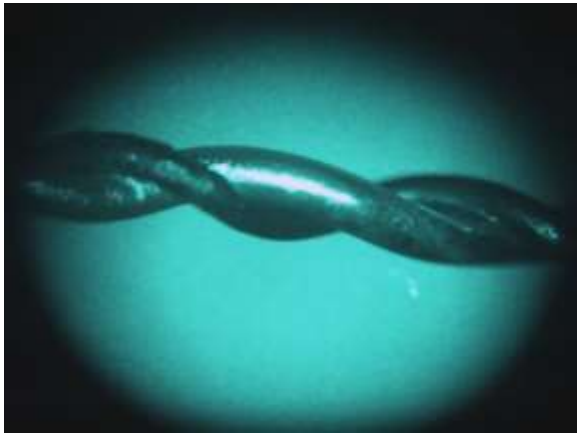

In collaboration with our colleagues from TSC, Tomsk

Шлирен метод

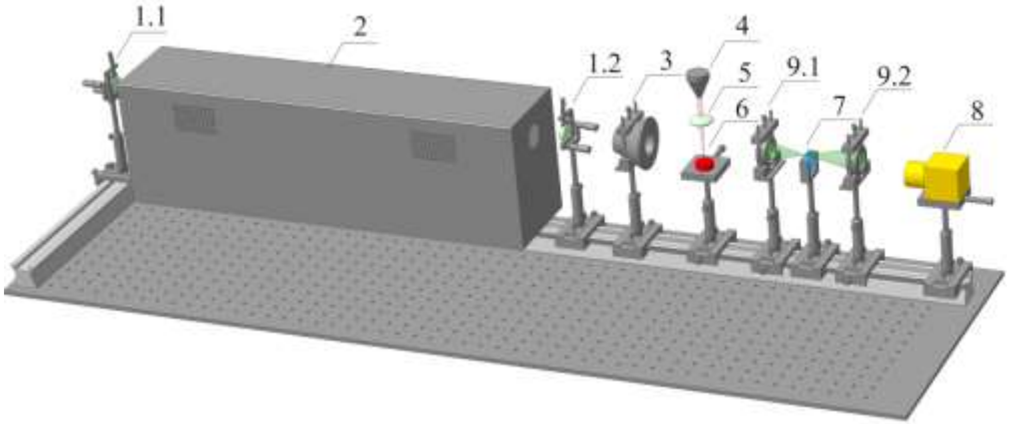

Visualization of a spark discharge in an atmosphere of various buffer gases.
Current pulse duration 50us.
The frame is formed by 1 or 2 pulses of CuBr laser radiation

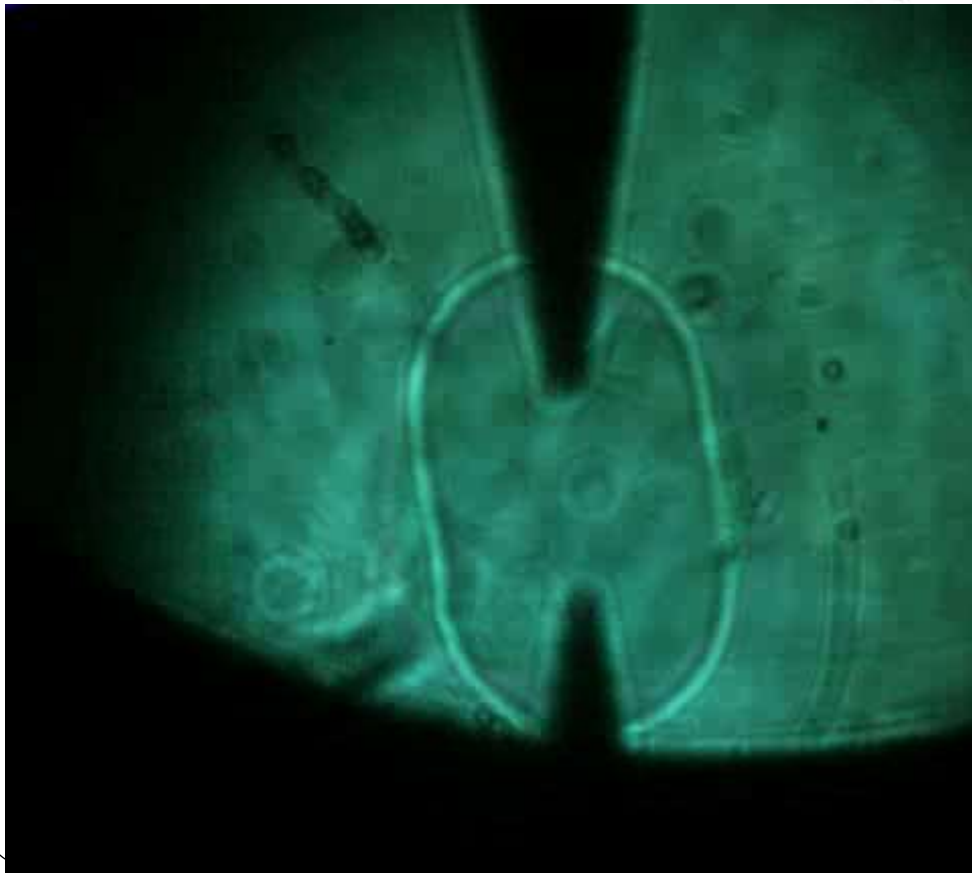

Schlieren method

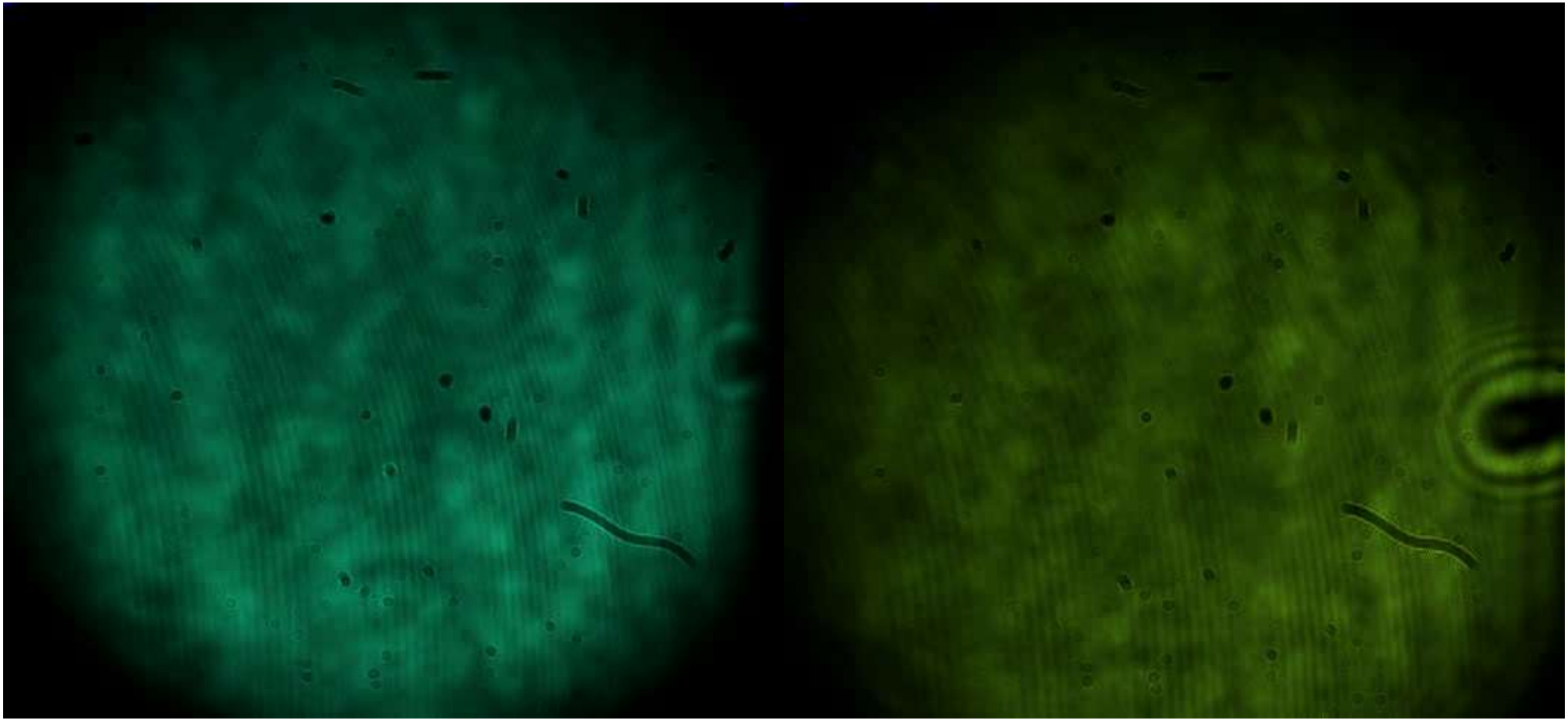

Nd:Y_2O_3, reflected, 3us

F shooting = 2100 frames/sec.